CHAPTER-4
MODELING AND CONTROL OF MULTIPURPOSE SINGLE STAGE GRID TIED THREE PHASE PHOTOVOLTAIC SYSTEM

With the advancement in technology, the recent past has seen the increasing use of photovoltaic (PV) generation in the power grid, ultimately resulting in reducing costs of power electronic devices in addition to various subsidies and encouragement schemes to promote solar generation. [1]. As increased nonlinear loads on the Distribution end of power sector have resulted in adversely affecting the operation and control of power grid along with higher instability [2]. In order to address these difficulties, grid tied PV system has introduced enhanced control techniques in frequency and time domain to control fluctuating load current thereby improving power quality. The frequency control technique deployed more computation burden as well as one cycle delay due to a window sampling method [3]. Hence, it is not appropriate for real time control application. A detailed analysis of the basic SRFT based control technique in a PV system reveals satisfactory results during balanced loading conditions [4]. However, in case of unbalanced load, dominance of third harmonic component was observed due which the performance of SRFT decreased drastically [4-5]. Hence to obtain a steady state response during unbalanced load, very low frequency is to be set for Low –pass filter (LPF) which in turn decreases the dynamic response of the PV system thereby giving it a stable condition [6]. To confront earlier mentioned issues, researchers have presented simple to complex various control approaches to ensure desire steady state as well as transient response [7]. References [5][9-12] have presented compressive and comparative review on a PV system with different control approaches to ensure superior steady state and dynamic response during ideal and non-ideal grid situations. Hence, by feeding maximum active power and minimum reactive power, grid reliability is obtained. Also an abrupt change in the solar irradiance causes DC-bus voltage fluctuations. To counter balance this, Feedback linearization technique is used to keep the DC voltage derivation within the acceptable limit.

The active power injected into the grid is proportionate to the availability of solar irradiance [16]. Reactive power control strategies such as frequency control, voltage regulation at PCC, power factor control at grid side etc. are accentuated due to modified control strategies of PV system which is described in [16-17]. Some of the important characteristics of grid tied PV system are simple design, efficient control mechanism, improved efficiency and reliable operation with the reduced cost in the application of PV inverter. Thus, the single-stage three phase grid tied PV inverter is an amiable and feasible option to fulfill almost above requirements with comparatively lower cost by eliminating a DC to DC converter for regulation of DC-bus voltage [17]. An insight into varied MPPT techniques along with various PV converter topologies (voltage source) are discussed in the references [16-17] [19-20]. Additionally, while ignoring the aspect of stability, various control techniques for single-stage PV system are described in the references [9][20-23][25]. Alternative way to utilize remaining capacity of PV inverter[18], quadrature axis current control is employed to the PV inverter by using a fixed value reactive power as per the safety rating of PV inverter However, if PCC voltage remains below the acceptable lower limit of PCC voltage for more than a prescribed period of time, then DERs need to be disconnect A unique concept of utilizing PV system as STATCOM at reduced load (or night hours) with additional various grid support functions. Furthermore, the unutilized inverter capacity after real power generation can be address by modifying control system during peak load (daytime) without oversizing PV inverter [19][18][20][22][26].

4.1 Architecture of PV system

According to power processing stage Photovoltaic (PV) inverters can be divided into the two categories: (i) Two-stage grid tied PV system, and (ii) Single-stage grid tied PV system[3]. In general, the output voltage of a PV array is not high enough and fluctuates with the changing ambient conditions, which is undesirable. As a result, an additional DC-DC converter stage is required[10][86], which ensures a constant DC-bus voltage regardless of changes in the input voltage. Despite the fact that the two-stage architecture provides advantages in controller design, it also has significant shortcomings. Increased circuit stages (DC-DC converter stage) cause an increase in power loss, which causes the overall energy transfer efficiency to drop [26]. Increasing the number of circuit stages also increases the complexity of the system, which results in decrease in system reliability. The active power flow of PV system is controlled by voltage source converter through maintaining DC-bus of PV inverter. However, two-stage PV system has a DC-DC converter for Maximum power extraction (i.e. first stage) and voltage source inverter for grid synchronization and power control (i.e. Second stage), which needs several additional power devices and components which cause considerable conduction losses, sluggish transient response and also increase cost. In order to improve system efficiency, the sub-control system like a MPPT algorithm, current control loop, and voltage control loop should only rely on the inverter, as illustrated in Figure 4-1.

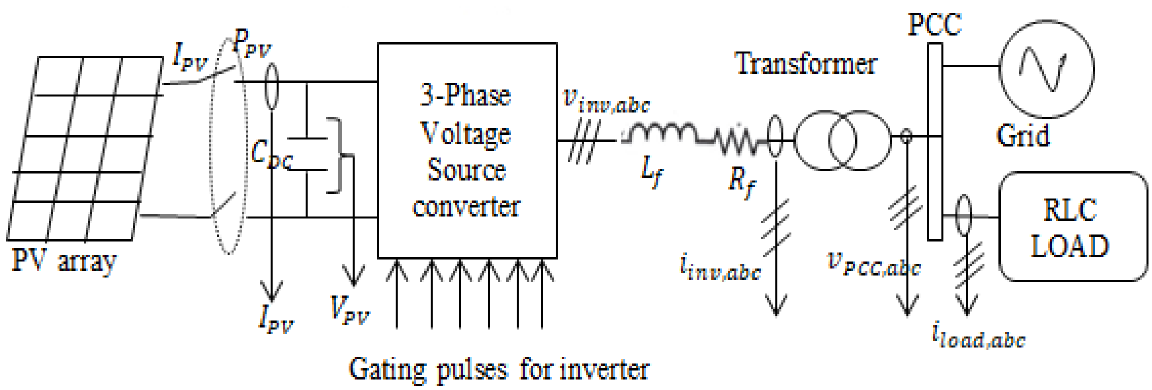

Figure 4- 1 : A power circuit diagram of single stage grid tied PV system

A boost converter for Maximum power extraction (First stage) and voltage source inverter for grid synchronization and power control (Second stage), which needs several additional power devices and components cause considerable conduction losses, sluggish transient response, and also increase the cost. The single-stage PV system is employed with the benefits of good efficiency and low-cost solution, as depicted in Figure 4-1. The drawbacks of the single-stage converter are that the PV panels are in series, and if the shading occurs on one or several PV panels, the whole system's efficiency is reduced. Over the day, the temperature and the solar irradiance level will change gradually as sunlight angles or shading patterns change, making gradual changes in PV characteristics and also, sometimes, quick changes in curves for just a short period may occur due to circumstances like passing birds or clouds. [7]. It is noted that the power and current of the PV module increase as increases solar irradiance level, in turn, and the MPP voltage will increase while the temperature is inversely proportional to the voltage and power of the PV panel, which means the open-circuit voltage and the MPP voltage decrease as increases temperature. Hence, MPPT control is necessary for maximizing the power generation PV systems. The two primary challenges of the grid-tied inverter, directly or indirectly, are the control of the DC-bus voltage (in the absence of a DC-DC converter) and controlling the AC power. The direct power control of grid-tied inverter can be achieved by applying instantaneous power theory, stationary frame control theory, or synchronous reference frame control theory, as depicted in Figure 4-2, for controlling current and/or voltage. However, the chapter also focuses on the DC-bus voltage management since the absence of a DC-DC converter stage between the PV panels and the grid, i.e., system controls depend only on voltage source converter. If the current control loop is absent, then the control is linear in terms of the decoupling between AC and DC dynamics but nonlinear in terms of the AC dynamics represented directly in terms of power. Direct power control can be achieved using a separate PWM modulator or without one (i.e., hysteresis current control).

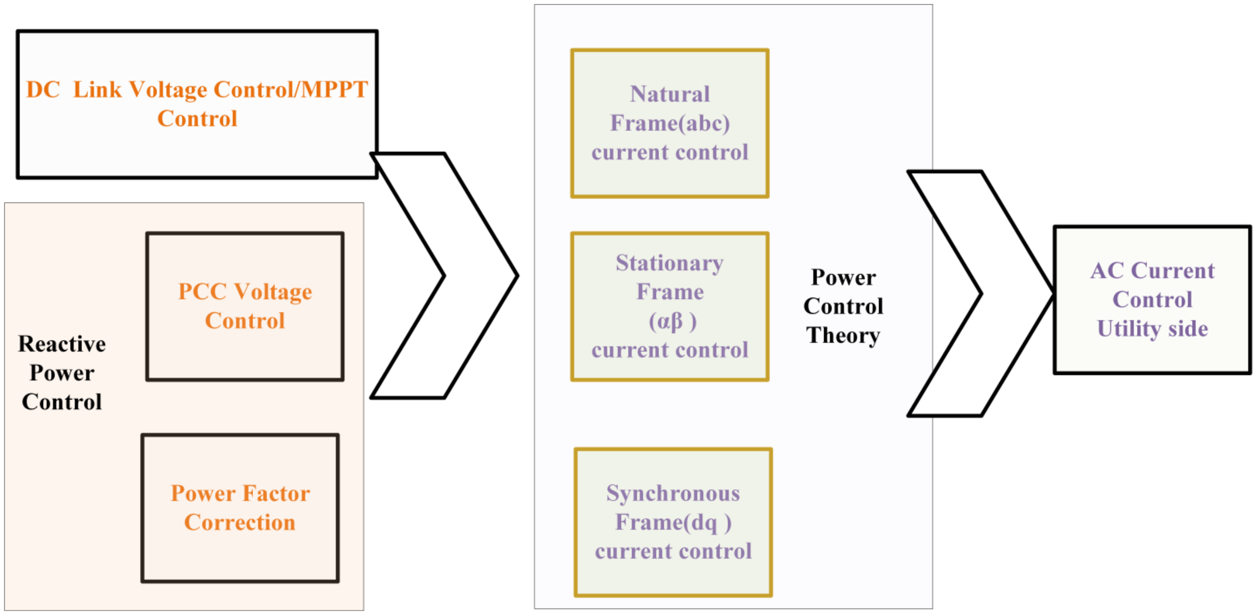

Figure 4- 2 : Conceptual Power theory for grid tied PV system

There are various current reference generation theories for a conventional PV system, STATCOM, and shunt active filter either in the discrete-time or frequency domain. The current reference generation theories in the frequency domain are Fourier series theory, Discrete Fourier transforms approach, Fast Fourier transform theory, recursive discrete Fourier transform, Kalman filter-based control algorithm. In contrast, the current reference generation theories in the time domain are Unit Template theory, Instantaneous reactive power theory, Synchronous reference frame theory, Instantaneous symmetrical component theory[3][5][8][13][28].

4.2 Synchronous Reference Frame Power Control of Single Stage Grid Tied Photovoltaic System

The principle of power exchange can be clarified using a short-line model having impedance ($z = R_f + j\omega L_f$) between voltage source converter ($v_{inv,abc}$) and the grid ($v_{pcc,abc}$) and, as shown in Figure.4-1.The control structure is depicted in the figure 4-3 and the dynamics mathematical expression for the single line model is given as:

$$\vec{V}_{inv,abc} = R_f \vec{i}_{inv,abc} + L_f \frac{d\vec{i}_{inv,abc}}{dt} + \vec{V}_{PCC,abc} \tag{4.1}$$

For the synchronous reference frame, abc→dq transformation is employed using the Park Transformation matrix and it is described as:

$$C_k = \sqrt{\frac{2}{3}} \begin{bmatrix} \cos\omega t & \sin\omega t & \frac{1}{\sqrt{2}} \\ \cos(\omega t - 120^0) & \sin(\omega t - 120^0) & \frac{1}{\sqrt{2}} \\ \cos(\omega t + 120^0) & \sin(\omega t + 120^0) & \frac{1}{\sqrt{2}} \end{bmatrix} \tag{4.2}$$

The matrix property is used here:

$$C_k^{-1} = C_K^T \tag{4.3}$$

The equation (4.1) is written in simplified manner:

$$\begin{bmatrix} v_{inv_a} \\ v_{inv_b} \\ v_{inv_c} \end{bmatrix} - \begin{bmatrix} v_{pcc_a} \\ v_{pcc_b} \\ v_{pcc_c} \end{bmatrix} = \begin{bmatrix} L & 0 & 0 \\ 0 & L & 0 \\ 0 & 0 & L \end{bmatrix} \frac{d}{dt} \begin{bmatrix} i_{inv_a} \\ i_{inv_b} \\ i_{inv_c} \end{bmatrix} + \begin{bmatrix} R & 0 & 0 \\ 0 & R & 0 \\ 0 & 0 & R \end{bmatrix} \left[\begin{bmatrix} i_{inv_a} \\ i_{inv_b} \\ i_{inv_c} \end{bmatrix} \right] \tag{4.4}$$

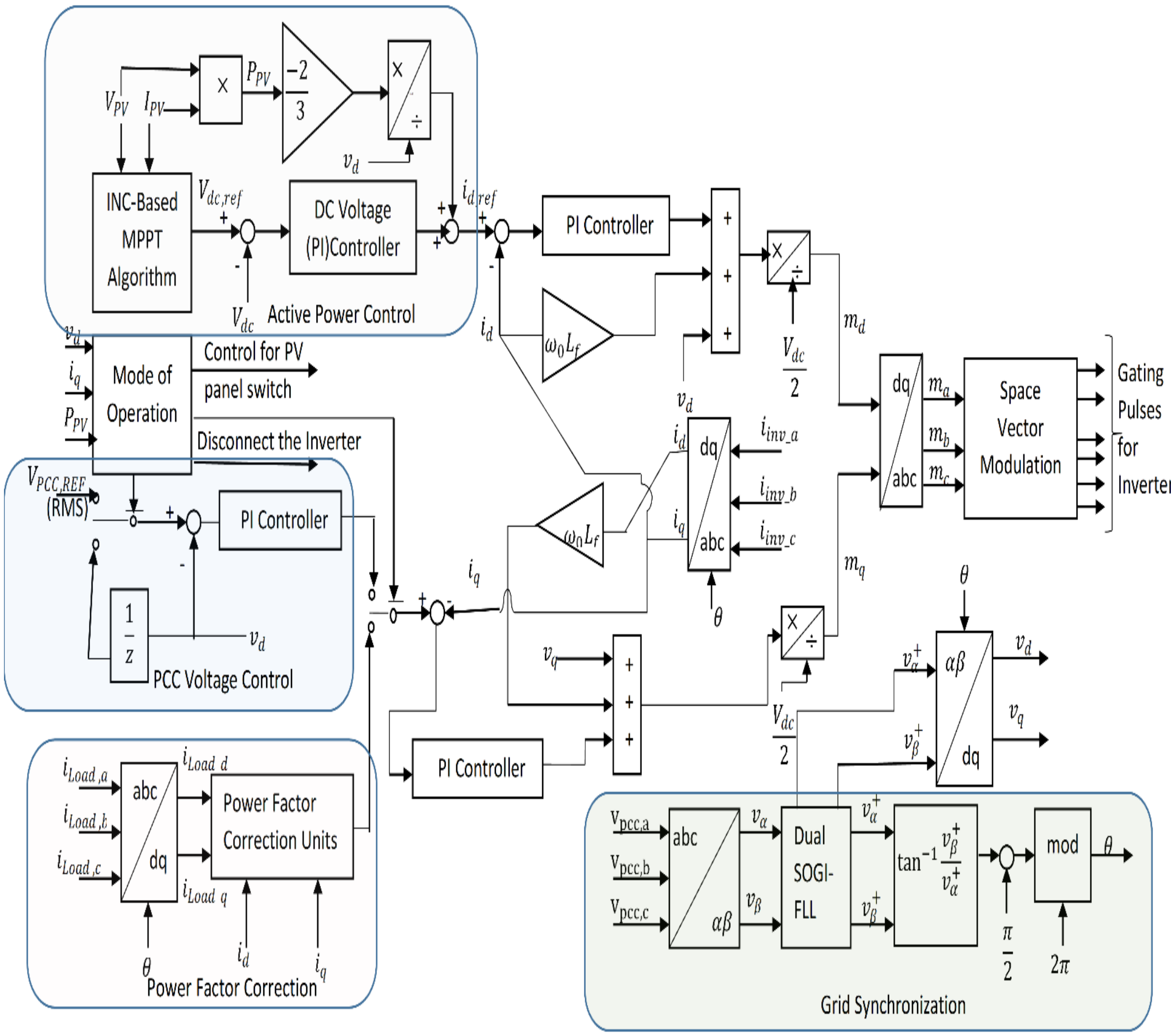

Figure 4- 3 : Control mechanism of single stage grid tied PV system in Synchronous reference frame

In the equation (4.4), abc →dq transformation is employed using the Park Transformation matrix and is described as:

$$[C_k]\left[v_{inv_{dq}} - v_{pcc_{dq}}\right] = [L]\frac{d}{dt}\{[C_k][i_{dq}]\} + [R]\{[C_k][i_{dq}]\} \tag{4.5}$$

The First term of equation (4.5) is simplified and represented as:

$$\frac{d}{dt}\{[C_k][i_{dq}]\} = [C_k]\frac{d}{dt}\{[i_{dq}]\} + [i_{dq}]\frac{d}{dt}\{[C_k]\} \tag{4.6}$$

By substituting the equation (4.2) into the equation (4.6), the differentiation of park-transformation is simplified as:

$$\frac{d}{dt}\{[C_k]\} = \sqrt{\frac{2}{3}}\begin{bmatrix} -\sin\omega t & \cos\omega t & 0 \\ -\sin(\omega t - 120^0) & \cos(\omega t - 120^0) & 0 \\ -\sin(\omega t + 120^0) & \cos(\omega t + 120^0) & 0 \end{bmatrix}\omega \tag{4.7}$$

By using trigonometry properties, Equation (4.7) can be simplified as:

$$\frac{d}{dt}\{[C_k]\} = \sqrt{\frac{2}{3}}\ \omega\begin{bmatrix} \cos\omega t & \sin\omega t & \frac{1}{\sqrt{2}} \\ \cos(\omega t - 120^0) & \sin(\omega t - 120^0) & \frac{1}{\sqrt{2}} \\ \cos(\omega t + 120^0) & \sin(\omega t + 120^0) & \frac{1}{\sqrt{2}} \end{bmatrix}\begin{bmatrix} 0 & 1 & 0 \\ -1 & 0 & 0 \\ 0 & 0 & 0 \end{bmatrix} \tag{4.8}$$

Here, a matrix M is assumed as:

$$[M] = \begin{bmatrix} 0 & 1 & 0 \\ -1 & 0 & 0 \\ 0 & 0 & 0 \end{bmatrix} \tag{4.9}$$

Hence, the equation (4.8) can be re-written as:

$$\frac{d}{dt}\{[C_k]\} = \omega[C_k][M] \tag{4.10}$$

The equation (4.5) is simplified and re-written as:

$$[C_k]\ \left[v_{inv_{dq}} - v_{pcc_{dq}}\right] = [L][C_k]\frac{d}{dt}\{[i_{dq}]\} + [L][i_{dq}]\frac{d}{dt}\{[C_k]\} + [R]\{[C_k][i_{dq}]\} \tag{4.11}$$

$$[C_k]\ \left[v_{inv_{dq}} - v_{pcc_{dq}}\right] = [L][C_k]\frac{d}{dt}\{[i_{dq}]\} + \omega[L][i_{dq}][C_k][M] + [R]\{[C_k][i_{dq}]\} \tag{4.12}$$

$$\left[v_{inv_{dq}} - v_{pcc_{dq}}\right] = [L]\frac{d}{dt}\{[i_{dq}]\} + \omega[L][M][i_{dq}] + [R]\{[i_{dq}]\} \tag{4.13}$$

Equation (4.13) can be simplified in context of d-axis and q-axis current:

$$[L]\frac{d}{dt}\{[i_d]\} = \omega[L][i_d] - [R]\{[i_d]\} + \left[v_{inv_d} - v_{pcc_d}\right] \tag{4.14}$$

$$[L]\frac{d}{dt}\{[i_q]\} = -\omega[L][i_q] - [R]\{[i_{dq}]\} + \left[v_{inv_d} - v_{pcc_d}\right] \tag{4.15}$$

The above proved equations (4.14) and (4.15) are the modeled inverter equations which contains the cross-coupled terms. So it can be observed that control of the output parameters is not possible directly by controlling d axis and q-axis separately. As it is a non-linear term, so, the decoupling is added to linearize the cross-coupling terms as well as to achieve control over two axes individually[7][44][46]. The overall amount of active component of reference current (d-axis reference current) is calculated by adding together the output of the proportional– integral (PI) controller and feed- forward PV current value. The simplified and well-known control theory is used to minimize error using the PI controller and assumed actual quantity as x. The difference between a reference quantity (x*) and an actual quantity (x) can be used to calculate the output of the PI controller, as shown in the following equation.

$$\varepsilon_x(m) = x^*(m) - x(m) \tag{4.16}$$

The error acquired from equation (4.16) is passed to the PI controller to obtain reference signal for the control system and described as:

$$x_{ref}(m) = k_p\, \varepsilon_x(m) + k_i \int_0^{T_s} \varepsilon_x(m)dt \tag{4.17}$$

The discretization of above equation, with the sampling time (T_s), can be obtained by converting integration into summation and represented as:

$$x_{ref}(m) = k_p\, \varepsilon_x(m) + k_i \sum_{k=0}^{m} \varepsilon_x(j)T_s \tag{4.18}$$

At sampling instant i.e. m=1, the equation can be represented as:

$$x_{ref}(1) = k_p\, \varepsilon_x(1) + k_i\{ \varepsilon_x(0) + \varepsilon_x(1)\}T_s \tag{4.19}$$

Similarly, at sampling instant, i.e. m=2 would be represented as:

$$x_{ref}(2) = k_p\, \varepsilon_x(2) + k_i\{ \varepsilon_x(0) + \varepsilon_x(1) + \varepsilon_x(2)\}T_s \tag{4.20}$$

The difference of reference quantity at consecutive instant is represented as:

$$x_{ref}(2) - x_{ref}(1) = \{ k_p\, \varepsilon_x(2) + k_i\{ \varepsilon_x(0) + \varepsilon_x(1) + \varepsilon_x(2)\}T_s\} - \{k_p\, \varepsilon_x(1) + k_i\{ \varepsilon_x(0) + \varepsilon_x(1)\}T_s \} \tag{4.21}$$

The simplification is given as:

$$x_{ref}(2) = x_{ref}(1) + k_p\, \{\varepsilon_x(2) - \varepsilon_x(1)\} + k_i\{ \varepsilon_x(2)\}T_s \} \tag{4.22}$$

Similarly, for m^{th} sampling instant, the reference quantity is described as:

$$x_{ref}(m) = x_{ref}(m-1) + k_p\, \{\varepsilon_x(m) - \varepsilon_x(m-1)\} + k_i\{ \varepsilon_x(m)\}T_s \} \tag{4.23}$$

Similarly, as equation(4.25), the reference quantity of the d-axis current is cumulative of power loss component and feed forward path, and computed by outer DC voltage control loop(Figure 4-3)as follow:

$$i_{d_{ref}}(n) = i_{d_{ref}}(n-1) + k_P \{(V_{dc_{ref}}(n) - V_{dc}(n)) - (V_{dc_{ref}}(n-1) - V_{dc}(n-1)\} + k_i T_s \{V_{dc_{ref}}(n) - V_{dc}(n)\} + \frac{2V_{PV}I_{PV}}{3V_m} \quad (4.24)$$

The active and reactive power flowing into the short-line model by assuming ($X_f = j\omega L_f \gg R_f$) can be computed as:

$$P = \frac{3}{2}[(V_d I_d) + (V_q I_q)] \quad (4.25)$$

$$Q = \frac{3}{2}[(-V_d I_q) + (V_q I_d)] \quad (4.26)$$

The Phase lock loop unit maintain V_d as peak value of PCC or grid voltage and V_q to the zero. Hence, consequently, the equation (4.25) and equation (4.26) are re-written as:

$$P = \frac{3}{2}(V_d I_d) \quad (4.27)$$

$$Q = \frac{3}{2}(-V_d I_q) \quad (4.28)$$

From equation (4.27) and equation (4.28), the active and reactive power output of inverter can be controlled through I_d and I_q, respectively, at certain PCC or grid voltage[7].

4.3 MPPT Extraction from PV Panel

The PV array delivers maximum power at a single operating point on the PV array characteristics for given fix isolation and temperature. The objective of maximum power point tracker is to detect the single operating point at which PV array can deliver maximum power irrespective of variations in solar isolation and temperature. The perturb and observe (P&O) and incremental conductance (INC) methods are well-known popular MPPT algorithm described in the literature [10][54-58][90-94]. The perturb and observe MPPT algorithm is robust and simple for the implementation on other hand has limitation to track correct maximum power point

(MPP) in rapidly changing atmospheric conditions. Hence, in this proposed work, INC MPPT algorithm is used engaged to identify maximum power point on a PV curve for further creation of the DC reference voltage, which is used in a control system for single- stage grid assisted system. It is worth pointing that the derivative of PV power with respect to its terminal voltage across PV array is result to null at maximum power point (MPP) on the power curve of PV[10][90][93].

The PV power and derivative of PV power with the PV voltage are mathematically written as:

$$P_{pv} = I_{pv} \times V_{pv} \tag{4.29}$$

$$\frac{\Delta P_{pv}}{\Delta V_{pv}} = \frac{\Delta(I_{pv} \times V_{pv})}{\Delta V_{pv}} = I_{pv} + V_{pv}\frac{\Delta(I_{pv})}{\Delta V_{pv}} \tag{4.30}$$

At MPP, it becomes zero and re-written as:

$$\frac{1}{(V_{pv})} \times \frac{\Delta P_{pv}}{\Delta V_{pv}} = \frac{I_{pv}}{V_{pv}} + \frac{\Delta(I_{pv})}{\Delta V_{pv}} = G_{pv} + \Delta G_{pv} = 0 \text{ (at MPP)} \tag{4.31}$$

where $G_{pv} = \frac{I_{pv}}{V_{pv}}$ and $\Delta G_{pv} = \frac{\Delta(I_{pv})}{\Delta V_{pv}}$ are represented as PV conductance and incremental conductance of PV respectively. From the equation (4.31), there are three operating points to determine the direction in which to climb based on the sign of $\Delta G_{pv} = \frac{\Delta P_{pv}}{\Delta V_{pv}}$ to reach MPP on a power curve of PV array and represented as:

$$\left.\begin{array}{c} G_{pv} + \Delta G_{pv} > 0 \text{ (Left side of MPP, climb upward);} \\ G_{pv} + \Delta G_{pv} = 0 \text{ (at MPP);} \\ G_{pv} + \Delta G_{pv} < 0 \text{(Right side of MPP, climb downward)} \end{array}\right\} \tag{4.32}$$

Figure 4-4 depicts the flow chart of the operating conditions of the Incremental-conductance MPPT algorithm and the PV characteristic of the PV panel. The primary advantage of the algorithm when compared to Perturb & observe (P&O) algorithms is that it is fast-tracking of the MPP deprived of oscillations with improved accuracy. Although, the time taken for computation in the Incremental-conductance MPPT algorithm is more due to its complexity. The speed of tracking of MPP is directly proportional to the step size in INC MPPT-the bigger the step size, the faster the monitoring. But, the problem with fast-tracking is that the significant power wave keeps oscillating around the MPP value and never attains exact MPP value.

(a)

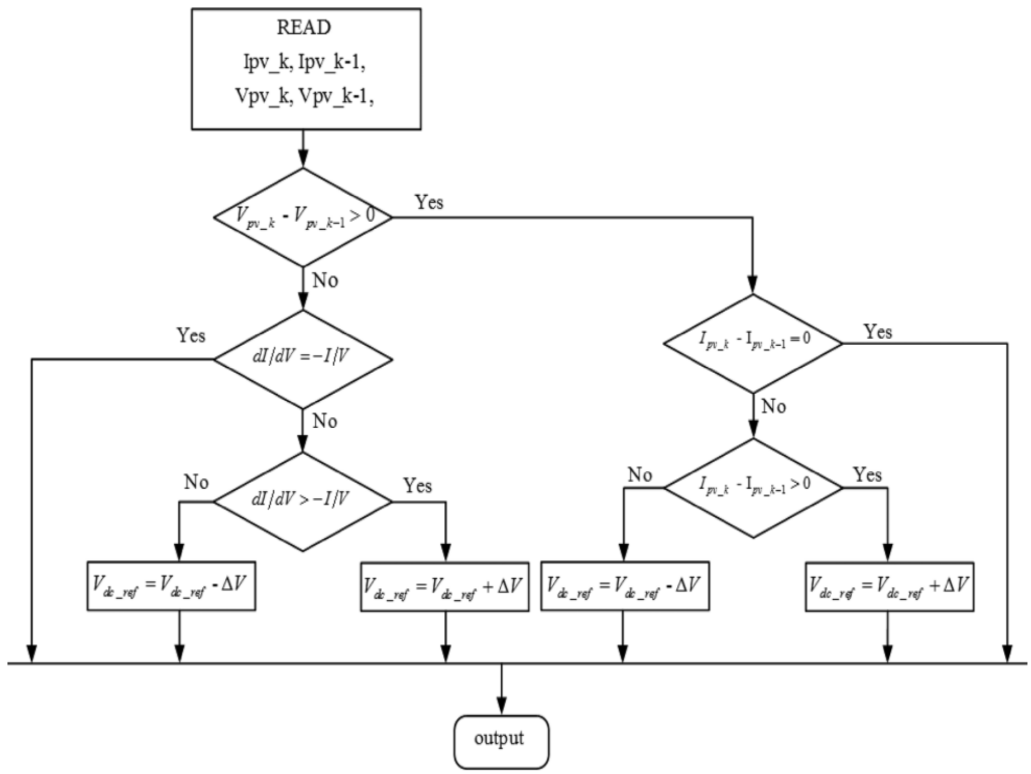

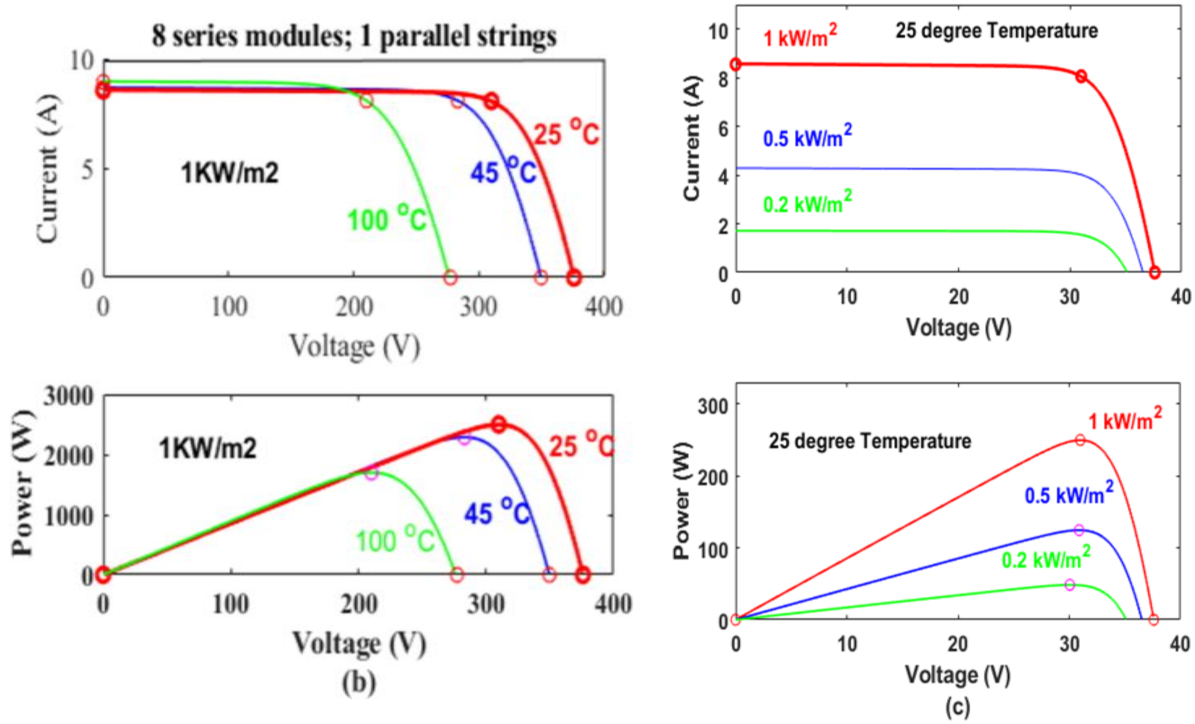

Figure 4- 4 : Flow-chart of Increment-conductance MPPT algorithm,(b) PV characteristic of PV panel with different temperature, and (c) PV characteristic of PV panel with different solar irradiance

This ultimately leads to lower efficiency. Whereas, when the step-size in the INC MPPT is small, the time taken to reach MPP value is more but greater accuracy and efficiency is observed. Thus, a choice between dynamics and oscillation is to be made during the operation of MPPT technique [7] [17][19][29].

4.4 DC-Bus Voltage Control

The DC-bus capacitor plays essential role to compensate inverter switches power loss by providing active power. As counter effect, voltage of DC-bus capacitor decays gradually, hence, small amount of active power needed which is absorbed by inverter to maintain a voltage of DC-bus capacitor. During day time a sufficient amount of solar irradiance available, DC-bus capacitor charged from PV panels to maintain DC-bus voltage and rest of the power injected into the grid. The DC-bus capacitor voltage is kept constant during the night by absorbing a minimal amount of active power from the grid through inverter diodes. When the MPPT Algorithm computes$V_{dc,ref}$, it uses the DC-bus voltage controller to maintain that voltage on the DC-bus capacitor.

The Energy stored in DC-bus capacitor is given as:

$$\Delta E = \frac{1}{2} CV^2 \tag{4.33}$$

The PI controller is employed to maintain DC-bus voltage in line with the MPP reference voltage, $V_{dc,ref}$, which is computed from MPPT algorithm.

The Power balance equation can be written as:

$$\left.\frac{\Delta E}{\Delta t}\right|_{t\to 0} = \frac{dE}{dt} = \Delta P = P_{PV} - P_{inv} \tag{4.34}$$

It can control the active power delivered into the grid by regulating the DC-bus voltage by changing the direct axis current. With the inverter power loss ignored, the power balance of both sides of the inverter in a steady-state should result in DC-bus power,P_{PV},equal to the output power at the AC-side terminals of VSC, which is equivalent to the output power at the grid, with the filter power loss ignored.

According to the power balance theory, the DC-bus capacitor's voltage dynamics are as follows:

$$\frac{d(\frac{1}{2} CV_{dc}^2)}{dt} = P_{PV} - P_{inv} \tag{4.35}$$

As per Synchronous reference frame (dq frame), The Power of inverter (P_{inv}) can be described as:

$$P_{inv} = \frac{3v_d i_d}{2} \tag{4.36}$$

By substituting equation (4.36) into (4.35), the power balance equation can be modified as :

$$CV_{dc}\frac{d(V_{dc})}{dt} = I_{PV} * V_{dc} - \frac{3v_d i_d}{2} \quad ; \quad \Rightarrow C\frac{d(V_{dc})}{dt} = I_{PV} - \frac{3v_d i_d}{2V_{dc}} \tag{4.37}$$

$$C\frac{d(V_{dc})}{dt} = I_{PV} - \frac{3v_d i_d}{2V_{dc}}$$

Here, i_d and v_d are the d-axis grid current and voltage respectively. It is a first order non-linear equation which should be converted into linear form for sake of simplicity in the control system. Consider a non-linear system, which is represented by functions f(x)and b(x) with control state x and given as

$$\dot{x} = f(x) + b(x) * u_i \tag{4.38}$$

Here, u_i is control input and described as:

$$u_i = \frac{1}{b}\{y - f(x)\} \tag{4.39}$$

Now, inserting equation (4.39) within equation (4.38), the non-linear system can be represented as linear system as

Hence, Non-linearity can be eliminated as:

$$\dot{x} = y \tag{4.40}$$

Similarly, substituting the $i_d = \frac{2v_{dc}}{3V_d}\{I_{PV} - y\}$ as control input, the equation (4.37) can be modified in the linearized differential form

$$C\frac{d(V_{dc})}{dt} = y \tag{4.41}$$

Therefore, the plant transfer function is described as

$$G_p(s) = \frac{V_{dc}(s)}{v_i(s)} = \frac{1}{sC} \tag{4.42}$$

A discrete PI controller is employed before plant transfer function to achieve a desired settling time and other dynamics parameters. The sampling time of current control loop is chosen 10times larger than the sampling time of voltage control loop in order to decouple the current control and voltage control loop for the control system.

4.5 Reactive Power control

The reactive power is exchanged with grid through PV inverter to achieve the control objective either PCC voltage regulation or maintaining unity power factor at grid side. During the variation of PCC voltage from the acceptable range, the control objective of multipurpose PV inverter is only to provide reactive power support to maintain PCC voltage within acceptable ranges, and behaves as fully STATCOM. During a fully STATCOM operation, direct- axis current reference sets to the zero. The quadrature - axis current reference, which is generated by the PCC outer loop voltage controller, provides a reactive power support to maintained the PCC voltage (in fully STATCOME MODE) or regulate unity power factor at grid side (in Partial-PV and partial STATCOM mode) [17][19-20].

4.6 PCC Voltage Regulation

The PCC voltage may be varied away from acceptable ranges depending on the loading conditions i.e. load presents at PCC. Hence, it is the control objective to maintain PCC voltage within acceptable range during any loading conditions and load variation. From the Figure 4-1 and Figure.4-3, grid current and PCC voltage can be described as:

$$i_{g,abc} = i_{Load,abc} - i_{PV,abc} \tag{4.43}$$

$$V_{PCC,abc} = L_g \frac{di_{g,abc}}{dt} + v_{g,abc} \tag{4.44}$$

By neglecting a transient condition of MDSOGI-FLL, It should be pointed that v_q is maintained to the zero by MDSOGI-FLL, where as v_d gives the PCC voltage. Therefore, ignoring current of the shunt filter capacitor, the PCC voltage in dq frame is described as:

$$v_d = L_g\, \omega_o\, i_q - L_g\, \omega_o\, i_{Load,q} - L_g \frac{di_d}{dt} + L_g \frac{di_{Load,d}}{dt} + V_{peak} \tag{4.45}$$

The error of PCC voltage is computed as:

$$\varepsilon_{v_{PCC}} = v^*_{ref\ PCC}(t) - v_{PCC}(t) \tag{4.46}$$

The PI controller eliminates the error between reference value of PCC voltage (Peak value of phase voltage / R.M.S value of phase voltage) and actual value of Peak value of phase voltage/ R.M.S value of phase voltage, which is computed from sensed three-phase PCC voltages. The output of the PI controller gives the reference value of the quadrature-axis current, $i_{q_{ref}}$, and it is expressed as:

$$i_{q_{ref}} = k_p \, \varepsilon_{v_{PCC}} + k_i \int_0^{T_s} \varepsilon_{v_{PCC}} \, dt \tag{4.47}$$

At sampling time T_s, the discretise form of the equation (4.47) can be represented as:

$$\begin{aligned} i_{q_{ref}}(m) = \; & i_{q_{ref}}(m-1) + k_p\{\varepsilon_{v_{PCC}}(m) - \varepsilon_{v_{PCC}}(m-1)\} \\ & + \; k_i \, \varepsilon_{v_{PCC}}(m) T_s \end{aligned} \tag{4.48}$$

The PI controller is employed in voltage control loop to make the quadrature-axis reference current, consequently, used in the current control loop of inverter. The PCC voltage control loop has inner quadrature-axis current control loop. Hence, the sampling time of voltage control loop is 10-50 times larger than the current control loop for the decoupling.

4.6.1 Power Factor Correction

During the availability of reactive loads at the PCC, if and only if PCC voltage is within an acceptable range, then the inverter also provides reactive power support to maintain unity power factor at the grid side, simultaneously injecting active power into the grid. As v_q=0, the phase difference (δ) is angle between grid voltage (PCC voltage) and grid current and Power factor at grid side is calculated as

$$PF = \cos\delta \tag{4.49}$$

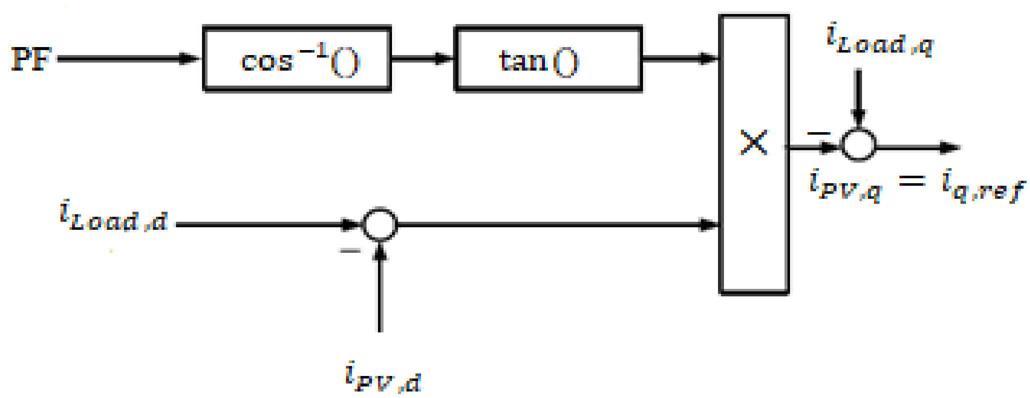

Figure 4- 5 : Block diagram for a Power factor correction

The relationship between quadrature axis inverter current and PF are derived as:

$$\tan\delta = \frac{i_{g,q}}{i_{g,d}} \; ; \qquad \tan(\cos^{-1} PF) = \frac{i_{Load,q} - i_{PV,q}}{i_{Load,d} - i_{PV,d}} \tag{4.50}$$

From the equation (4.50), to obtain desire power factor, the quadrature –axis reference inverter current is derived as:

$$i_{q,ref} = -1 \times \{ i_{Load,q} - \{\tan(\cos^{-1} PF) \times (i_{Load,d} - i_{PV,d})\}\} \tag{4.51}$$

The quadrature –axis reference inverter current is generated for unity power factor at grid by taking the value PF to be zero. For unity power factor, which means PF =1 that gives $(\cos^{-1} PF) = 0$ and equation (4.51) is re-written as:

$$i_{q_{ref}} = -\, i_{Load,q} \tag{4.52}$$

4.7 Current Control in synchronous reference frame

The dynamics of AC current in multipurpose inverter, as shown in single line diagram (Figure 4-1and Figure 4-3), is mathematically represented by following equations in d-q frame

$$L_f \frac{di_d}{dt} = -R_f i_d + \omega L_f i_q - v_{gd} + v_{inv,d} \tag{4.53}$$

$$L_f \frac{di_q}{dt} = -R_f i_q - \omega L_f i_d - v_{gq} + v_{inv,q} \tag{4.54}$$

For linearization as well as sake of simplicity, $v_{inv,d}$ and $v_{inv,q}$ are taken as:

$$v_{inv,d} = -\left[k_p + \frac{k_i}{s}\right] \times \left(i_{d,ref} - i_d\right) - \omega L_f i_q + v_{gd} \tag{4.55}$$

$$v_{inv,q} = -\left[k_p + \frac{k_i}{s}\right] \times \left(i_{q,ref} - i_q\right) + \omega L_f i_q + v_{gq} \tag{4.56}$$

The equation (4.53) and equation (4.54) are modified as:

$$L_f \frac{di_d}{dt} = -\left(R_f - \left[k_p + \frac{k_i}{s}\right]\right) i_d - \left(\left[k_p + \frac{k_i}{s}\right]\right) i_{d,ref} \tag{4.57}$$

$$L_f \frac{di_q}{dt} = -\left(R_f - \left[k_p + \frac{k_i}{s}\right]\right) i_q - \left(\left[k_p + \frac{k_i}{s}\right]\right) i_{q,ref} \tag{4.58}$$

Here, k_p and k_i are the proportional and integral gains of the PI controllers. A discrete PI controller is employed before plant transfer function to achieve a desired settling time and other dynamics parameters. The sampling time of voltage control loop is chosen 10-50 times larger than the sampling time of current control loop in order to decouple the current control and voltage control loop for the control system.

4.8 Mode Operation of PV-STATCOM

The control mode of operation is functioning according to an operating scenario as depicted in Figure 4-6. To evaluate the performance of a multipurpose single-stage PV system, the methodological approaches are used:(i) conventional PV operation in both forward and reverse power flow conditions, (ii) multipurpose PV inverter operation in "Partial STATCOM" mode for voltage regulation and power factor correction and, (iii) conventional STATCOM operation for voltage regulation and power factor correction. The PCC voltage is denoted by v_{pcc} in all simulation results. Grid currents, PV inverter currents and load currents are denoted by the variables i_{grid} , $i_{inverter}$and i_{Laod}, respectively. The effectiveness of the presented grid assisted PV system is demonstrated by the simulation results in Simulink/MATLAB environment.

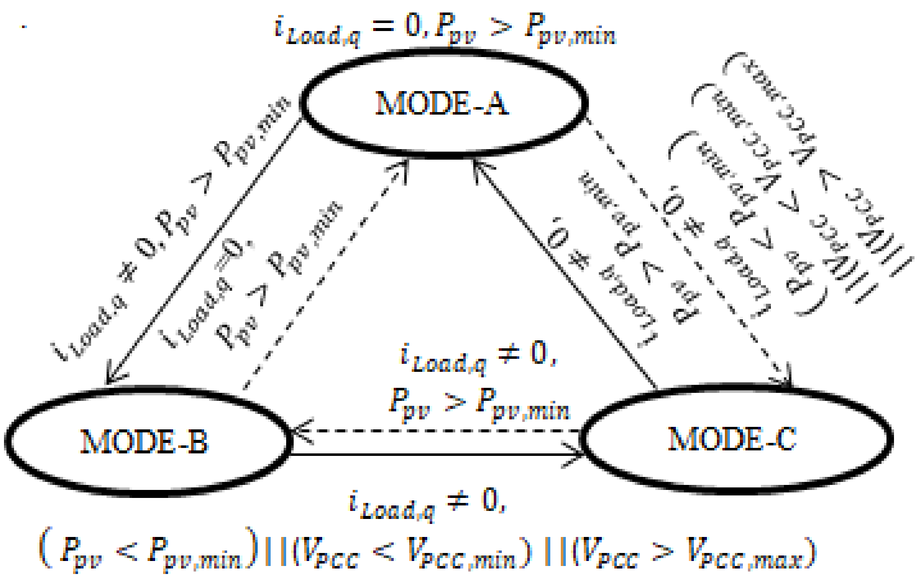

Figure 4- 6 : Control for mode of operation

The active and reactive power of PV inverter, load, and grid are denoted as: P_{inv}, Q_{inv}, P_{load}, Q_{load}, P_g,and Q_g, respectively.The presented control approach of inverter is modeled and designed as single-stage grid connected system with 2.5kW maximum power generation capacity of PV system at maximum power point (MPP) during 1000 $\frac{W}{m^2}$ solar insolation/irradiance. The dynamic performance assessment of presented control approach for grid assisted PV system is carried out for different modes of operation at various operating condition as follow:

4.8.1 Active Power injection mode [PV system only-day time, Conventional PV system]

The objective of this control mode is to inject maximum active power from PV panels as per available irradiance to the grid during day hours when the load is not attached to PCC. The quadrature axis reference current is set to a null value in this mode. The 1KW active power and1KVAR reactive power load is connected at PCC. Initially, the PV system is not connected at the PCC. The utility grid fulfills the power demand of load from t=0.3 seconds to 0.4 seconds, as depicted in Figure 4-7. At t= 0.4 seconds, the PV inverter is connected at PCC with 1200W power generation. Consequently, the surplus power (after fulfilling load demand) flows back to the grid source in the reverse direction. It needs more than one cycle for the PV inverter current to stabilize. The performance of a multipurpose single-stage PV system is summarized in the context of time to time action during reverse power flow in table 4-1.

Table 4-1: Summary of performance evaluation for multipurpose single stage PV system in Full-PV mode

Time (Seconds)	Action (PV panels)	Active Power (Watt)			Reactive Power(VAR)		
		PV Inverter	Grid (Receiving /Suppling)	Load Demand	PV Inverter	Grid (Receiving /Suppling)	Load Demand
0.3 to 0.4	disconnected	0	-1000	+1000	0	-1000	+1000
0.4 to 0.5	Connected	-1200	+200	+1000	0	-1000	+1000
0.5 to 0.6		-1600	+600	+1000	0	-1000	+1000
0.6 to 0.7	disconnected	0	-1000	+1000	0	-1000	+1000

(a)

(b)

(c)

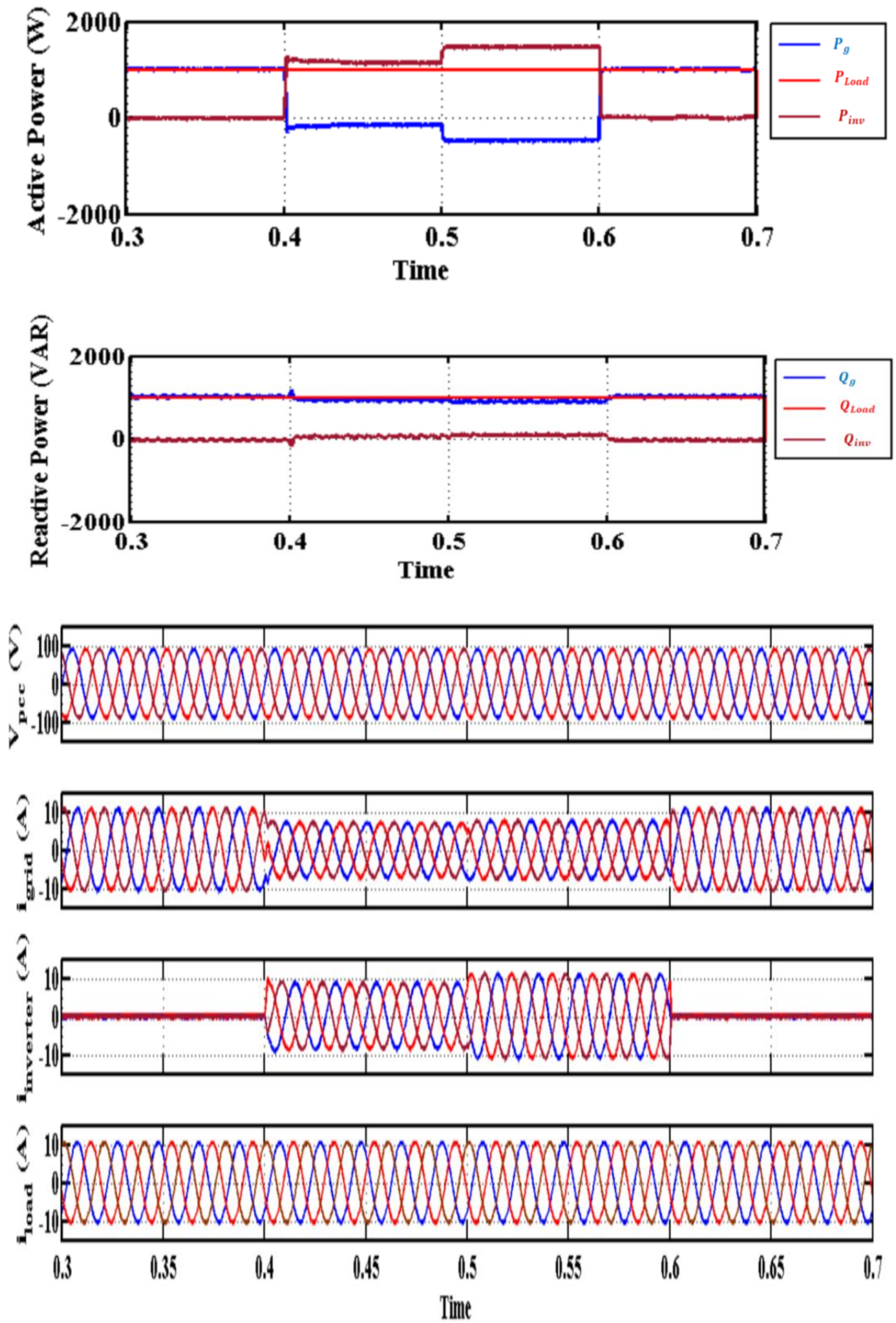

Figure 4- 7 : Dynamic performance of multipurpose single-stage PV system during full-PV mode (reverse power flow)

However, the abrupt power reversal at PCC results a transient on grid current and PCC voltage. At t=0.5 seconds, The PV panels increase their power generation from 1200 W to 1600W. These results in an increase in PV inverter currents i_{inverter} , consequently, increase the grid current i_{grid} increases in the opposite way as solar energy generation exceeds the required load power. The PV inverter is cut off from the PCC at t= 0.6 seconds. The PV inverter currents (i_{inverter}) instantly drop to zero and the entire load demand is supplied by the grid.

Table 4-2 : Summary of performance assessment for multipurpose single stage PV system in Full-PV mode (Forward power flow)

Time (Seconds)	Action (PV panels)	Active Power (Watt)			Reactive Power(VAR)		
		PV Inverter	Grid (Receiving /Suppling)	Load Demand	PV Inverter	Grid (Receiving /Suppling)	Load Demand
0.3 to 0.4	disconnected	0	-2000	+2000	0	-2000	+2000
0.4 to 0.5	connected	-1200	-800	+2000	0	-1000	+1000
0.5 to 0.6		-1600	-400	+2000	0	-1000	+1000
0.6 to 0.7	disconnected	0	-2000	+2000	0	-1000	+1000

The 2KW active power and 2KVAR reactive power load are connected at PCC. Initially, the PV system is not connected at the PCC. The utility grid fulfills the power demand of load from t=0.3 seconds to 0.4 seconds, as depicted in Figure 4-8. At t= 0.4 seconds, the PV inverter is connected at PCC with1200W power generation. Consequently, the 2KW load power demand is coordinately fulfilled by the PV inverter and utility grid. However, the grid current declines because more of the load can now be provided by PV power output. The utility grid provides the short of 800W load power demand, as described in table 4-2. At t=0.5 seconds, the PV panels increase their power generation from 1200 W to 1600W, increasing PV inverter currents.

(a)

(b)

(c)

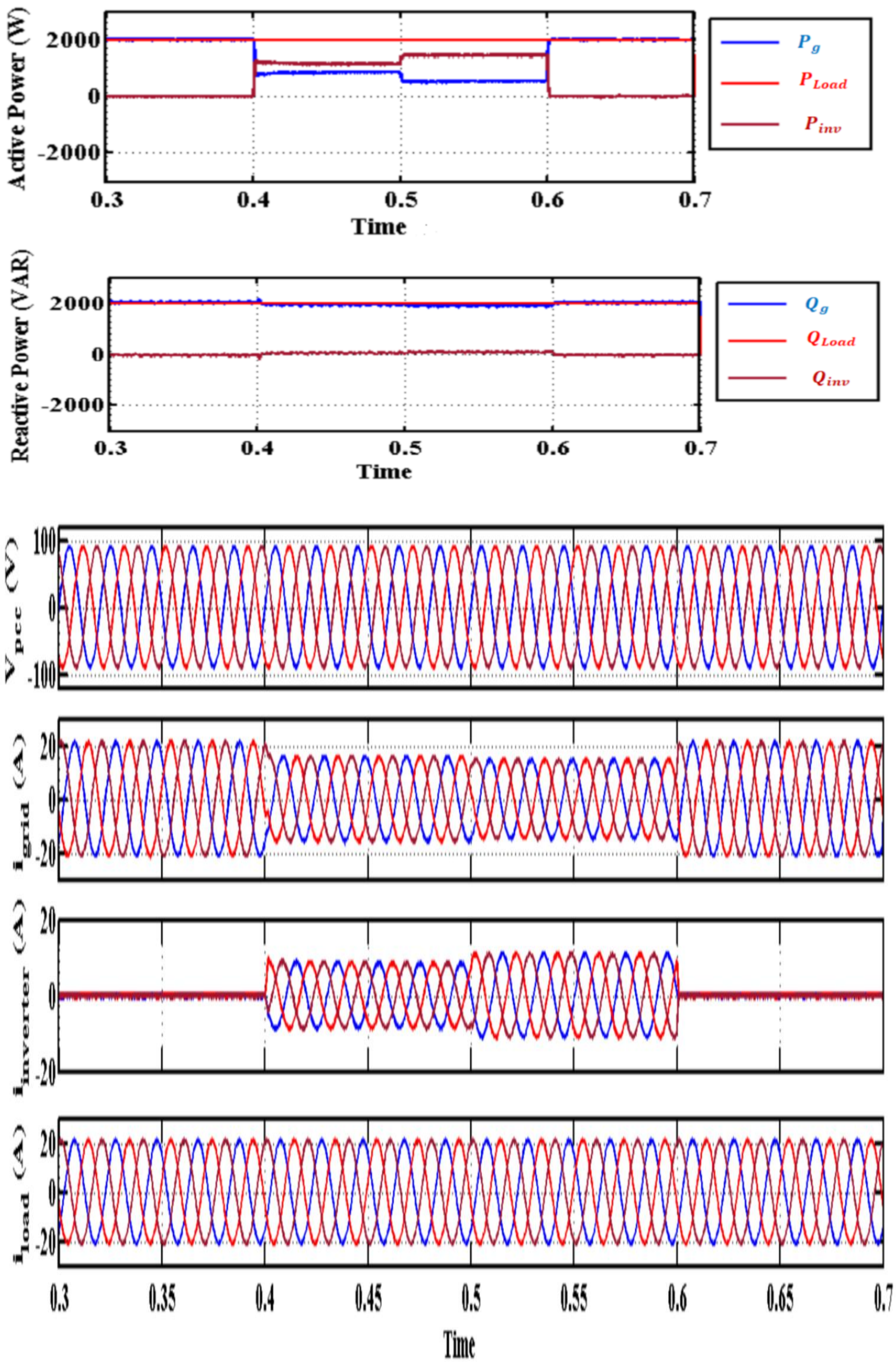

Figure 4- 8 : Dynamic performance of multipurpose single-stage PV system during full-PV mode (forward power flow)

Consequently, active power load demand from a utility grid is also reduced from 800W to 400W, as depicted in Figure 4-8. The PV inverter is cut off from the PCC at t= 0.6 seconds. The PV inverter currents instantly drop to zero, and the grid supplies the entire load demand. A gross forward power flows from the grid to load. The performance of a multipurpose single-stage PV system is summarized in the context of time to time action during forward power flow in table 4-2.

4.8.2 Active and Reactive Power injection mode [Partial PV & Partial SATCOM-Daytime MODE-B]

The objective of this control mode is to inject maximum active power from PV panels as per available irradiance to the grid, simultaneously ensuring unity power factor by providing reactive power support at the side of the utility grid when the reactive load is connected, an acceptable range of PCC voltage is sensed. The reactive power exchange with a utility occurs with the residual operating capacity of the inverter during this mode. Thus, it is also called the "Partial PV-STATCOM" mode. The performance of a multipurpose single-stage PV system is summarized in the context of time to time action as PV-STATCOM in table 4-3.

Table 4-3: Summary of performance assessment for multipurpose single stage PV system in PV-STATCOM mode

Time (Seconds)	Action (PV panels	Active Power (Watt)			Reactive Power(VAR)		
		PV Inverter	Grid (Receiving /Suppling)	Load Demand	PV Inverter	Grid (Receiving /Suppling)	Load Demand
0.3 to 0.4	connected	-1600	-200	+1800	-1200	+200	+1000
0.4 to 0.5		-1300	-700	+1800	-1519.86	+519.86	+1000
0.5 to 0.6		-1800	0	+1800	-871.78	-128.22	+1000
0.6 to 0.7	disconnected	0	-1800	+1800	0	-1000	+1000

In other words, the conventional PV system operates as a STATCOM utilizing its partial inverter capacity in the form of reactive power support to ensure unity power factor (Power factor correction, PFC mode) at the grid side during daytime.

(a)

(b)

(c)

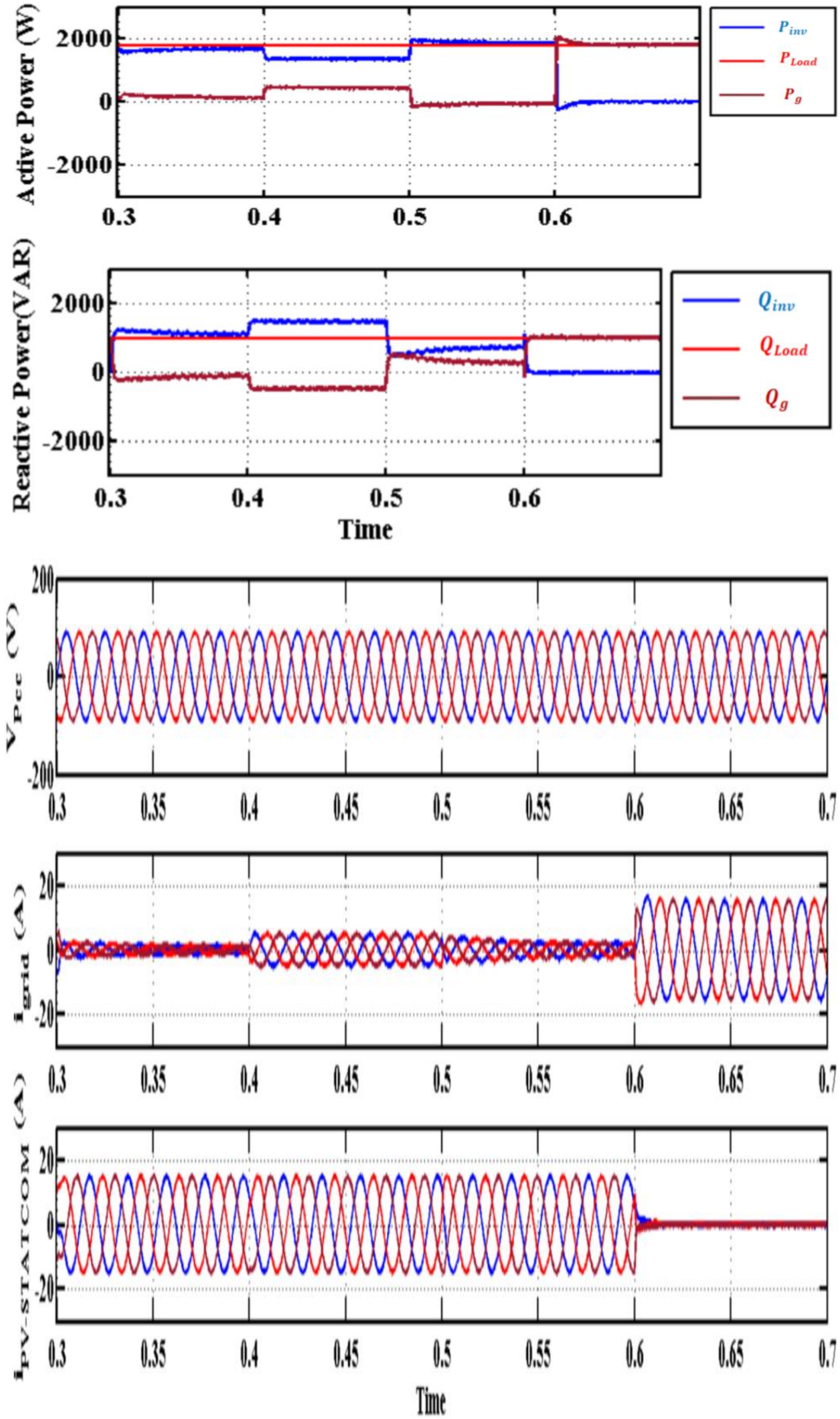

Figure 4- 9 : Dynamic performance of multipurpose single-stage PV system during Partial PV & Partial-STATCOM mode

The 1800W active power and 1000 VAR reactive power loads are connected at PCC. The dynamic performance evaluation of the multipurpose PV system is tabulated in table-4-3 from the waveform of active and reactive power of the grid, PV inverter, and loads, as depicted in Figure 4-9. The PCC voltages, grid currents, PV inverter currents, and load currents are observed for the performance assessment of multipurpose single-stage PV system, as depicted in Figure 4-9. The PV inverter is connected at PCC with1600W power generation at t= 0.3 seconds, 1300W at t= 0.4 seconds, and 1800W at t= 0.5 seconds. At t= 0.6 seconds, The PV inverter is disconnected from the PCC. The reactive power exchange with utility occurs with the residual operating capacity of PV inverter, i.e., 1200VAR at t= 0.3 seconds, 1519.86 VAR at t= 0.4 seconds, and 871.78VAR at t= 0.5 seconds. At t= 0.6 seconds, the PV inverter is disconnected from PCC, at which the utility grid fulfills the reactive power load demand.

4.8.3 Reactive power injection mode [STACOM-Night time, critical day hours, MODE-C]

This control mode ensures a PCC voltage within an acceptable range, i.e.,$\pm 5\%$ PCC voltage, during both direction power exchanges with utility, sometimes in the day. At night time, PCC voltage regulation is the highest priority; if the PCC voltage is fixed acceptable utility range, then the Secondary objective is to make a unity power factor for the grid. The multipurpose PV system is connected to utility and reactive loads at PCC. The 1800W active power and 1800 VAR reactive power loads are connected at PCC. The dynamic performance evaluation of the multipurpose PV system is tabulated in table-4-4 from the waveform of active and reactive power of the grid, PV inverter, and loads, as depicted in Figure 4-10. The PCC voltages, grid currents, PV inverter currents, and load currents are observed for the performance assessment of multipurpose single-stage PV system. The performance evaluation is carried out without PV-STATCOM (in FULL-STATCOM mode) and with PV-STATCOM (in FULL-STATCOM mode). During the test evaluation without PV-STATCOM (in FULL-STATCOM mode), the utility fulfills the reactive power load demand from t= 0.3 seconds to t= 0.4 seconds (or from t= 0.6 seconds to t= 0.7 seconds) and disconnected PV inverter from PCC.

(a)

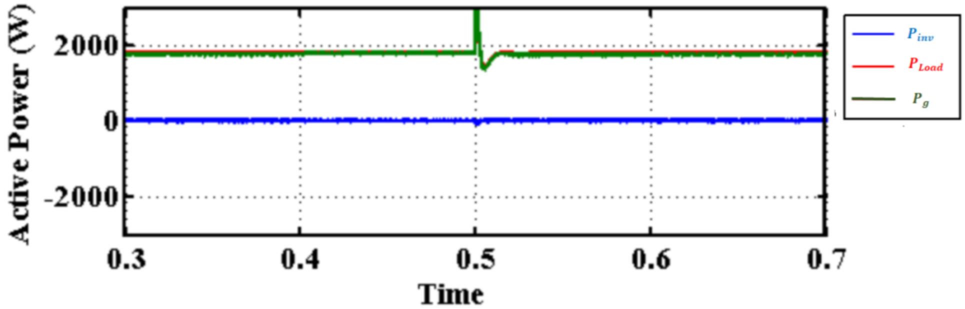

(b)

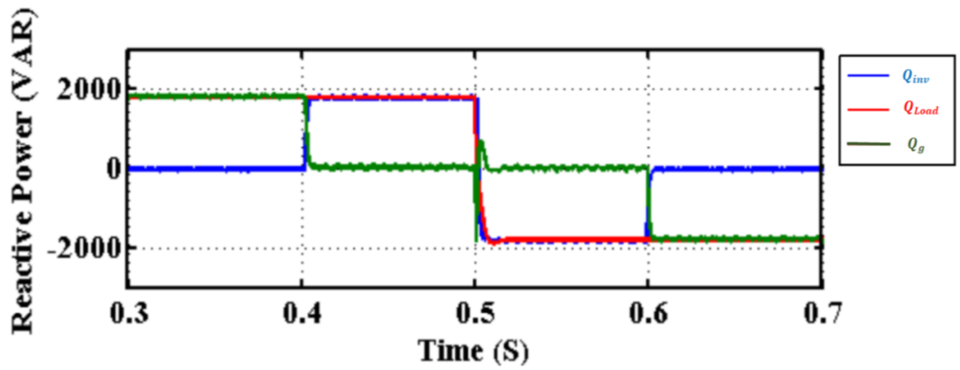

(c)

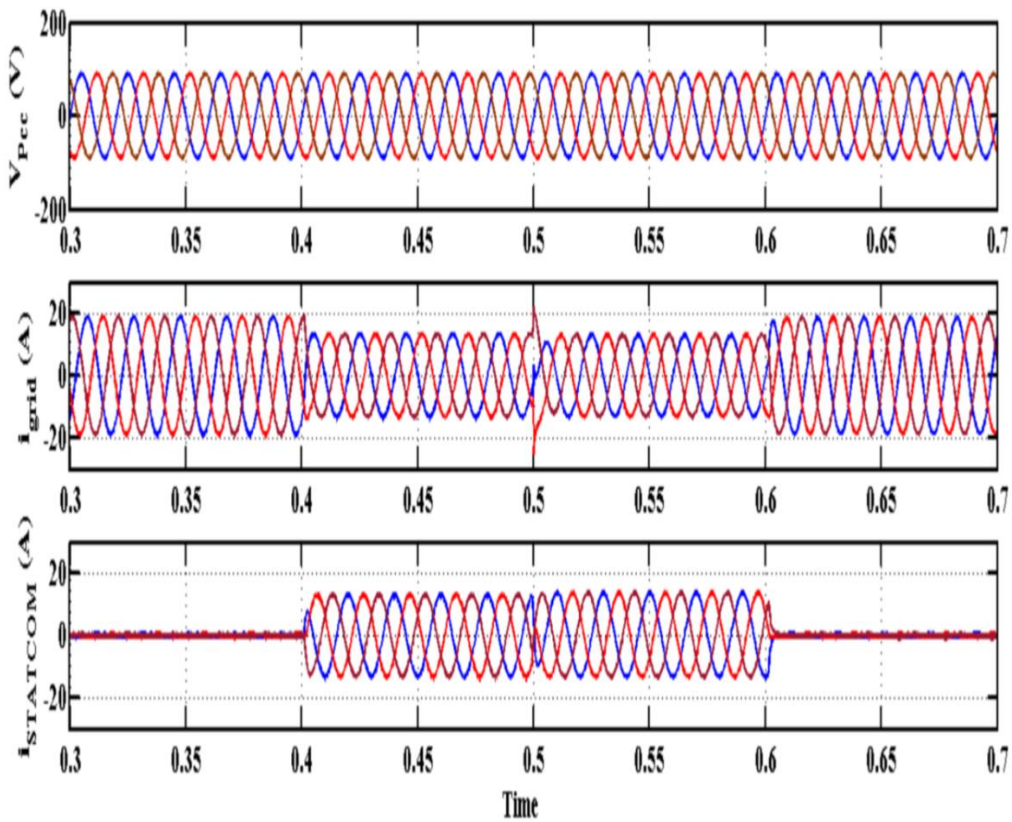

Figure 4- 10 : Dynamic performance of multipurpose single-stage PV system during Full-STATCOM mode

Table:4-4: Summary of performance assessment for multipurpose single stage PV system during Night time

Time (Seconds)	**Action** (STATCOM)	**Active Power (Watt)**			**Reactive Power(VAR)**			
		PV Inverter	**Grid (Receiving /Suppling)**	**Load Demand**	**PV Inverter**	**Grid (Receiving /Suppling)**	**Load Demand**	**Load Type**
0.3 to 0.4	disconnected	0	-1800	+1800	0	-1800	+1800	Inductive
0.4 to 0.5	connected	0	-1800	+1800	-1800	0	+1800	
0.5 to 0.6		0	-1800	+1800	-1800	0	+1800	Capactive
0.6 to 0.7	Disconnected	0	-1800	+1800	0	-1800	+1800	

During the test evaluation with PV-STATCOM (in FULL-STATCOM mode), the inductive type load and PV inverter are connected to the utility grid at PCC. In this test, the PV inverter fulfills the reactive power load demand from t= 0.4 seconds to t= 0.5seconds, and the PV inverter behaves as a capacitive type load. While the capacitive type load demand is fulfilled by PV inverter from t= 0.5 seconds to t= 0.6seconds and PV inverter act as inductive type load.

4.8.3.1 Power Factor Correction

The active load in this simulation is 1500W, whereas the reactive load is altered from inductive to capacitive. The reactive load is initially a 1500VAR inductive type load. Figures 4-11(a) and (b) illustrate the grid, load, and photovoltaic system active and reactive power changes due to load and photovoltaic power variations. Figure 4-11(c) shows the grid power factor, PCC voltage (v_{PCC}), and grid current (i_{grid}) for phase "A," in the multipurpose single-stage PV inverter's control target being power factor correction. The PV-STATCOM system is interfaced to the grid, and the control objective is set to PV mode at time t=0.3 seconds.

(a)

(b)

(c)

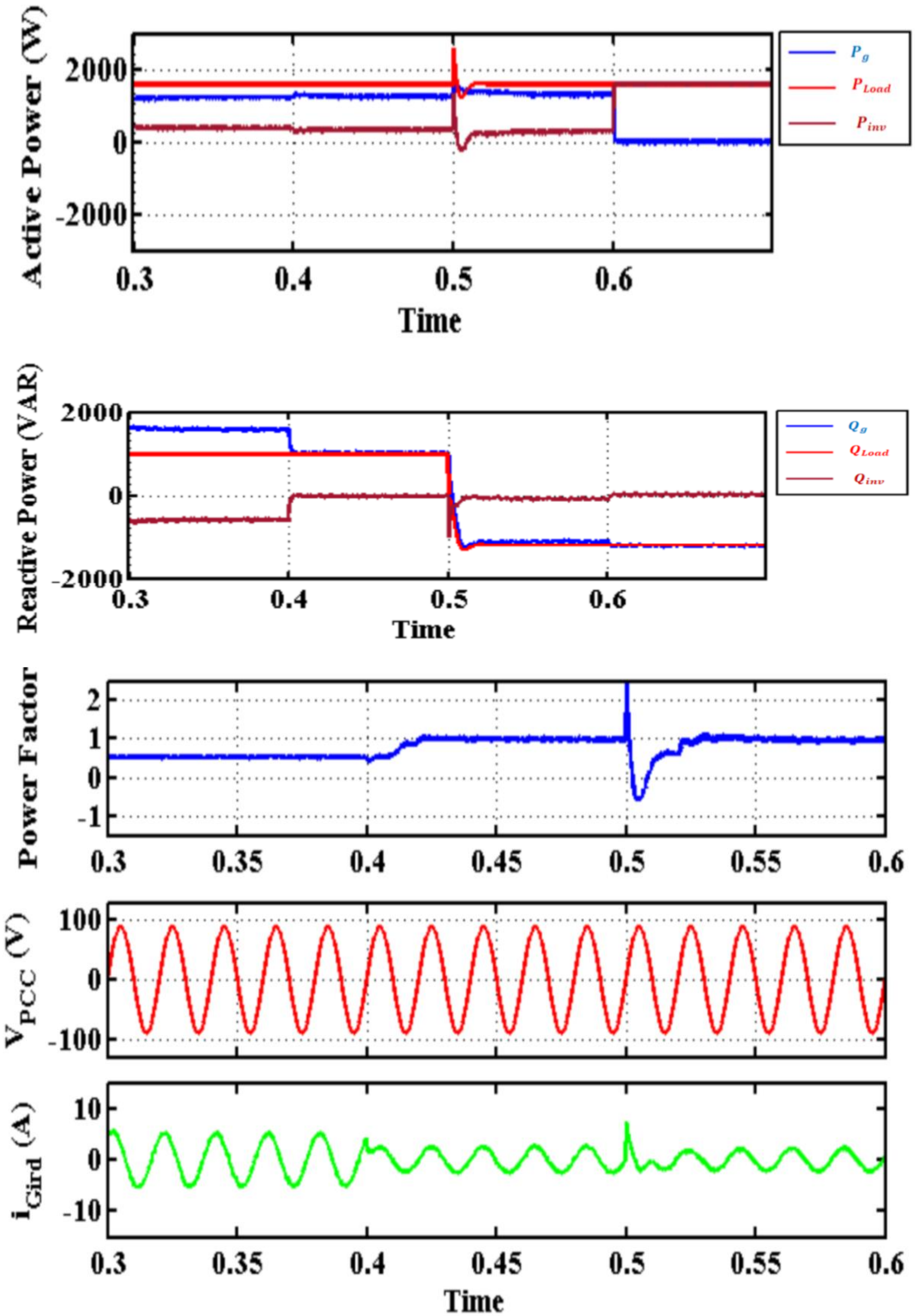

Figure 4- 11 : Dynamic performance of multipurpose single-stage PV system (PV-STATCOM) during power factor correction

The photovoltaic system output is 400W at this level.

When PV-STATCOM generates solely active electricity, the grid power factor is approximately 0.69. As a result, the voltage at the PCC (v_{pcc}) and the grid current (i_{grid}) are out of phase. The load active power (P_{Load}) is supplied by both the grid (P_{grid}) and a photovoltaic-STATCOM system ($P_{inverter}$), whereas the majority of the load reactive power (Q_{load}) is supplied by the grid (Q_{grid}).At t=0.4 seconds, the controller enters power factor correction mode and utilizes the remaining capacity of the inverter to restore the power factor to unity. The controller increases the grid power factor from 0.69 to unity. As a result, following a transient, the PCC voltage (v_{pcc}) and the grid current (i_{grid}) become phase-locked. PVSTATCOM exchanges reactive power equal to the reactive power needs of the load in order to enhance power factor. As a result, the reactive power of PV-STATCOM ($Q_{inverter}$), equals (Q_{load}), and the reactive power of the grid (Q_{grid}) decreases to zero. Additionally, the results indicate that improving the power factor of a multipurpose single-stage photovoltaic inverter has little effect on active power output. In other words, during power factor adjustment, the active power output of PV-STATCOM ($P_{inverter}$) maintains 400W. Thus, the successful decoupling of the active and reactive power controllers is proved.

4.9 Dynamic performance assessment of control approach for multipurpose single-stage grid connected system

The simulation results are carried out to conclude the effectiveness of the control approach for multipurpose single-stage grid-connected system in the following manner: During the daytime, Mode A is operated when the no-load or linear load is connected to the utility grid while Mode B is operated when the non-linear load is attached to the point of common coupling (PCC). In this section, the remaining capacity of the inverter is used to exchange reactive power in Mode B. Hence, this controller mode is also known as the “Partial PV-STATCOM” mode. In other words, the conventional PV system operated as a STATCOM utilizing its partial inverter capacity in the form of reactive power support to ensure unity power factor (Power factor correction, PFC mode) at the grid side during daytime. Figure 4-12 illustrate that the utility grid is only interfaced with PV inverter up-to time instant t=0.3

seconds, i.e., Mode A, the capacitive load is connected at the point of common coupling from the time instant t = 0.3 to 0.5 seconds, and the load shifted to inductive load after time instant t= 0.5 seconds. At t= 0.85 i.e., Mode B. The solar isolation/irradiance is varied from 1000 $\frac{W}{m^2}$ to 500$\frac{W}{m^2}$. from time instant t =0.3 to t =0.7 seconds, and again to 1000$\frac{W}{m^2}$ at t= 0.7 seconds. The non-linear load is shifted from Capacitive Load to inductive load with the rating P_{load}= 500W and Q_{load}= 1500VA at the time instant t =0.5 seconds to observe the dynamic stability of the system.

From simulation results depicted in Figure 4-12, it is observed that:

1. At time instant t $\leq$ 0.2 seconds, the multipurpose PV system operates active power injection mode(Mode A)and only inject active power (2500W)into utility grid at maximum power point using MPPT algorithm on the inverter, and inverter currents and PCC voltages are 180^{o}out of phase in the mode A. It is intentionally Mode A, and Mode B simulated sequentially to verify the performance of the control algorithm during no-load conditions to reactive load conditions.
2. At time instant between t= 0.3 seconds and t = 0.5seconds, the active power and the reactive power demand of capacitive load is entirely served by the multipurpose PV system and operated in active and reactive power injection mode (Mode B). Moreover, the surplus active power is injected into the grid after serving a capacitive load and ensures unity power at the utility. The active power injection is dependent on available solar irradiance and extracted maximum power from PV panels using the MPPT algorithm on the inverter. The PV system is connected to the grid and inductive type load with the rating rating P_{Load} = 500W and Q_{load} = (-1500VA) at the point of common coupling; at the same moment, solar irradiance varied from 1000 $\frac{W}{m^2}$ to 500$\frac{W}{m^2}$. Therefore, the PV system has generated 1200W (P_{inv})in which 500W power (P_{load}) delivered to the load and remaining power(P_{grid}) injected to the utility grid while need of negative reactive power(Q_{load}) to the load provided by the utility grid (Q_{grid}). The active power injection is reduced to the 1250W at time instant t=0.5 seconds, further, again increases to the 2500W at time instant t=0.65 seconds due to

change in solar irradiance from $1000\frac{W}{m^2}$ to $500\frac{W}{m^2}$, and again increases to $1000\frac{W}{m^2}$. Besides, the grid reactive power support and unity power factor at grid side are maintained along with main objective to inject active power as per availability of solar irradiance on the PV panels. In a single stage grid-tied converter, DC-bus voltage is maintained by the $V_{dc,ref}$, derived from maximum power point tracking (MPPT) algorithm during the conventional-PV mode or the Partial-PV & Partial-STATCOM mode operation.

3. At time instant between t= 0.5 seconds and t = 0.7seconds, the load is switched from capacitive load to inductive load type with the rating $P_{load} = 500W$ and Q_{load} = (+1500VA), instead of negative reactive power (Q_{load}) support, now, positive reactive power (Q_{load}) provided to the load from utility grid (Q_{grid}) rest of the events are identical.
4. At time instant t ≥0.7 seconds, the PV system is again generating 2500W (i.e. P_{inv}) due to the change in solar irradiance($500\frac{w}{m^2}$ to $1000\frac{W}{m^2}$), surplus active PV power injected to utility grid which causes the PCC voltage v_{pcc} to rise, resulting in a steady state rise in current i_{load} through constant impedance load, although after a transient. The inverter filter effectively removes the harmonics in the inverter current. The inverter current leads to load current during an inductive type load, whereas lags to load current during a capacitive type load for maintaining grid current at unity power factor in a grid side.
5. Modified DSOGI-FLL can eliminate both the harmonics distorted component (100Hz and 300Hz component) and negative sequence from and, further provided to tan-arc PLL block for the detection of phase-angle needed in synchronization of the control system.

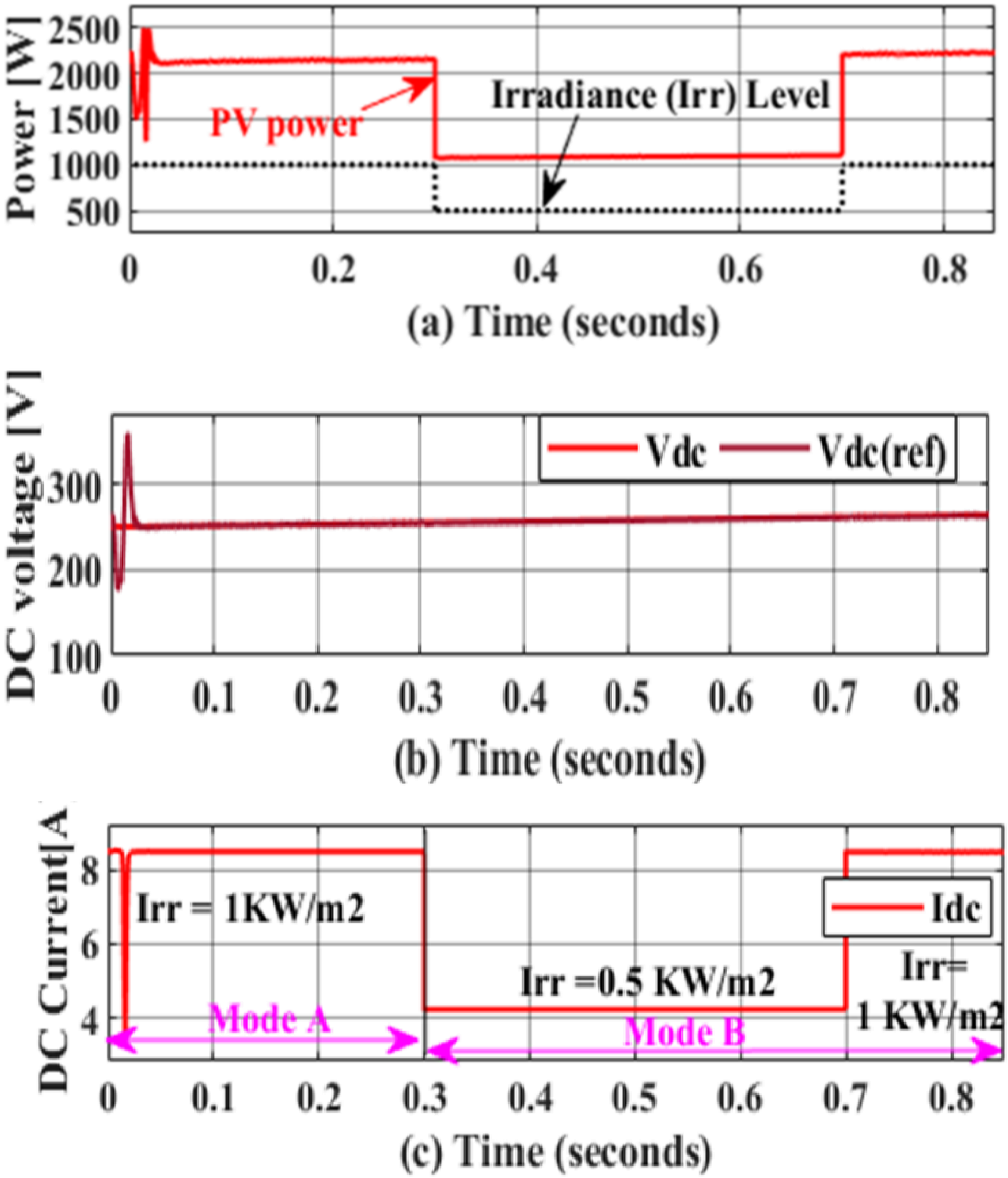
Power [W]
2500
2000
1500
1000
500
PV power
Irradiance (Irr) Level
0
0.2
0.4
0.6
0.8
(a) Time (seconds)
DC voltage [V]
300
200
100
Vdc
Vdc(ref)
0
0.1
0.2
0.3
0.4
0.5
0.6
0.7
0.8
(b) Time (seconds)
DC Current[A
8
6
4
Irr = 1KW/m2
Idc
Irr =0.5 KW/m2
Irr=
1 KW/m2
Mode A
Mode B
0
0.1
0.2
0.3
0.4
0.5
0.6
0.7
0.8
(c) Time (seconds)

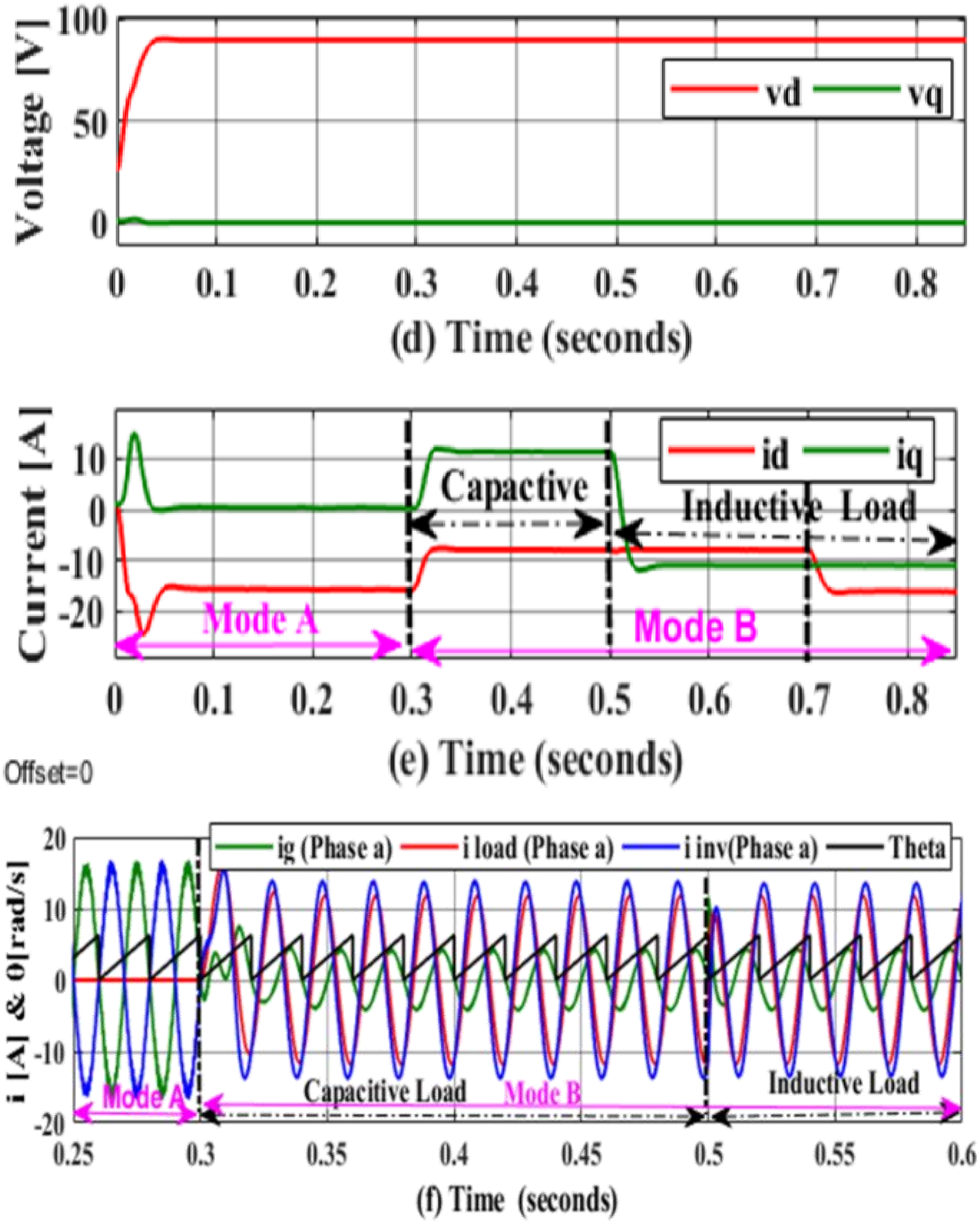

Figure 4- 12 : Simulation results of MODE A and MODE B
(a) P_{pv} (W)and Irriandance $\left(Irr,\frac{w}{m^2}\right)$,(b) V_{dc} and $V_{dc(ref)}$ (c) PV current (I_{dc}), (d) d-q axis PCC voltage, (e) d-q axis inverter current ,(f))grid current, inverter current , load current and theta.

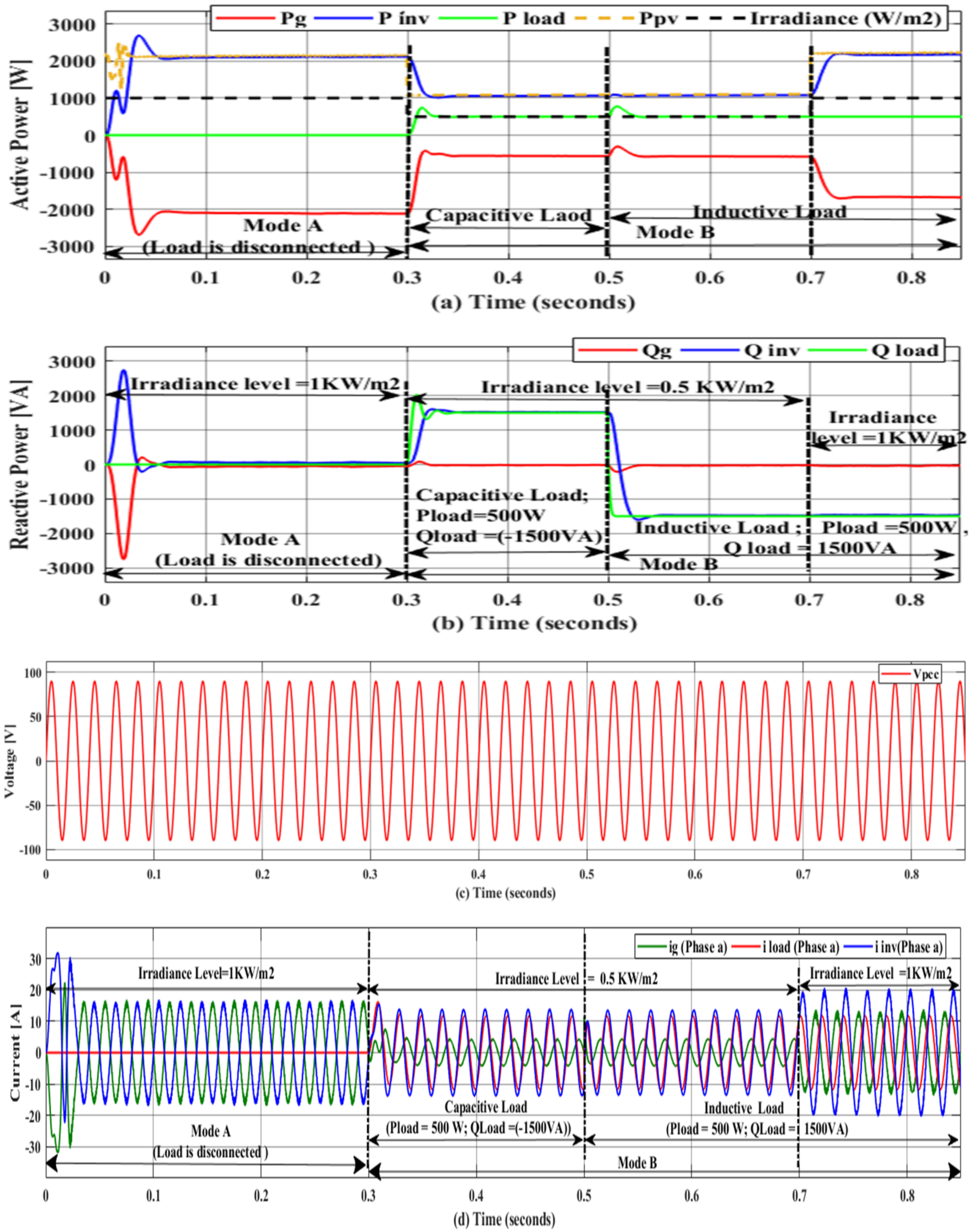

Figure 4- 13 : Simulation results of MODE A and MODE B(a)Active Power of P_g, P_{inv} and Irriandance $\left(Irr, \frac{w}{m^2}\right)$,(b) Reactive Power of Q_g , Q_{inv} , Q_{load} (c) PCC voltage (Phase a) and, (d)grid current, inverter current , load current.

The PV inverter gets disconnected from PV panels during the nighttime and entirely behaves as STATCOM. The control objectives of the system are to regulate PCC voltage as the main priority and power factor correction at the grid side when PCC voltage is in an acceptable range. The PCC voltage is reduced due to sizeable inductive type reactive load connected at PCC whereas increased due to either capacitive type reactive load connected at a PCC or active power injected in a grid. During the day, sometimes, PCC voltage is raised above the acceptable range of voltage due to the active power injection from a PV system, and the Multipurpose PV system is switched from Mode B to Mode C (Full STATCOM).

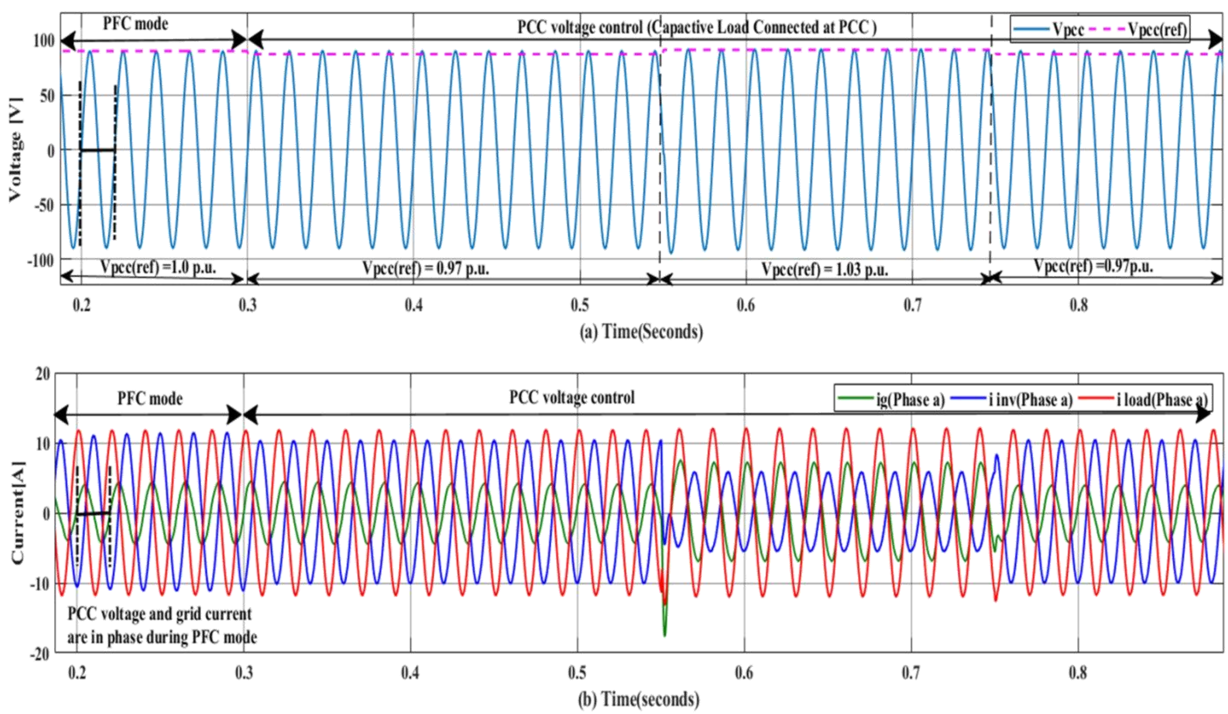

Figure 4- 14 : Simulation result of Multipurpose PV system connected to capacitive load at PCC (a) PCC voltage(Phase A), and (b) grid current(Phase A),, inverter current(Phase A), and load current(Phase A).

The proposed control approach detaches the PV panels from PV inverter in this condition and regulates PCC voltage with in an acceptable range in a one cycle by exchanging reactive power to the PCC. For validation control approach, The PCC Voltage reference is changed from 1.0 p.u. to 0.97 p.u at t =0.3 seconds, further varied from 0.97 p.u. to 1.03 p.u at t= 0.55 seconds, and again from 1.03 p.u to 0.97 p.u at a t= 0.75 seconds.

From simulation results depicted in Figure 4-14 and Figure 4-15, it is observed that:

1 At time t≤0.3 seconds, the multipurpose PV system functions in power factor correction mode due to PCC voltage in permissible limit i.e., 1.0 p.u. In PFC enabled MODE C, The PCC voltage and grid current are in phase to ensure unity power at a utility side.

2 At time 0.55 ≤ t ≤ 0.75 seconds, the reference PCC voltage is changed to 1.03 p.u. value and tracked PCC voltage within one cycle time. Again, PV inverter (PV-STATCOM) operated either in inductive mode if large capacitive load connected at PCC or capacitive mode for inductive load attached to PCC. It is noted that PV inverter (PV-STATCOM) phase currents are decreased to regulate PCC voltage as per the reference value if capacitive load connected at PCC, as depicted in Figure 4-14, whereas increased in a case of inductive load connected at PCC, as a depicted in Figure 4-15.

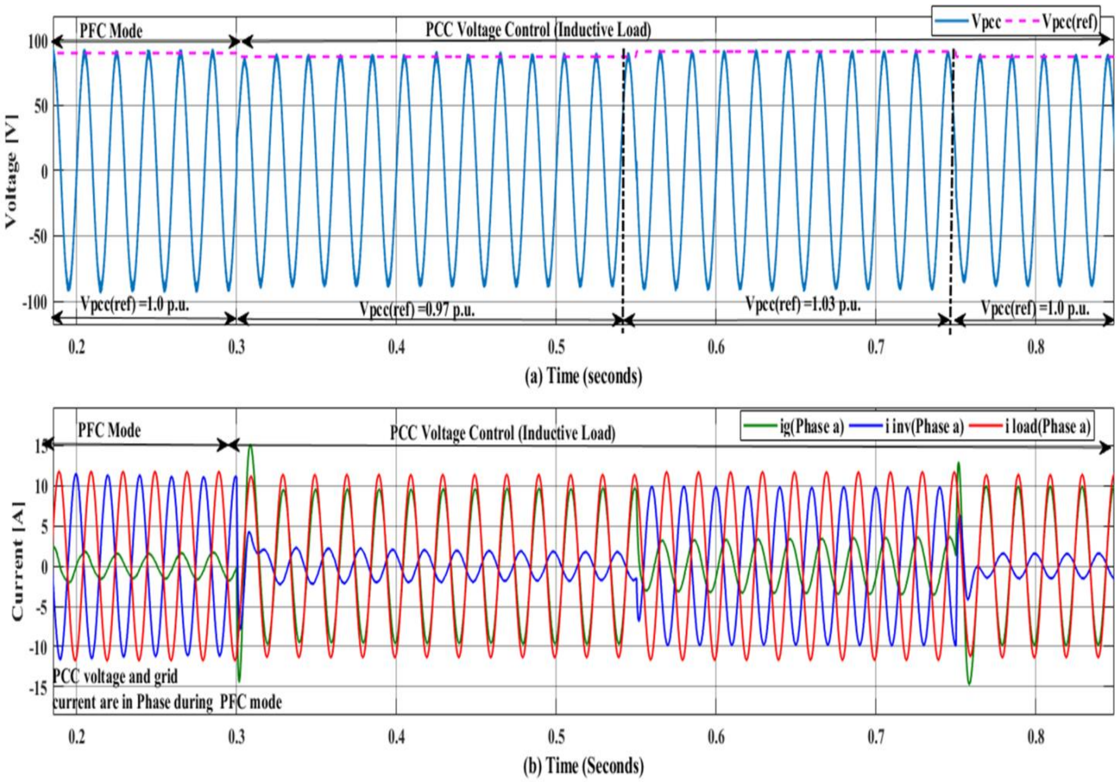

Figure 4- 15 : Simulation result of Multipurpose PV system connected to inductive load at PCC (a) Phase A of PCC voltage, and (b)phase A of grid current, inverter current, and load current

3 For the time $t \geq 0.75$ seconds, now, PV inverter (PV-STATCOM) phase currents is again increased in a case of capacitive load, as observed in Figure 4-14, and decreased during an inductive load, as observed in Figure 4-15, to regulate PCC voltage as per the reference value 0.97 p.u.

4.10 Hysteresis Current Controller

The most well-known method of hysteresis control is employed to control current in the single-stage PV system. Thus, the controller reacts rapidly to any deviation from control references, which explains its high gain characteristic. Note that the digital implementation of hysteresis control methods does not guarantee that the ripples in the control variable are within the bounds of a defined hysteresis band. Following that, a direct power control (DPC) for grid-connected applications was developed to directly manage the converter's active and reactive power by selecting the optimal switching state [36]. It has a simple and without PI controller current control structure. It cannot control additional constraints such as capacitor voltage balancing and switching frequency reduction. Moreover, it is not possible to multi-variable cases.

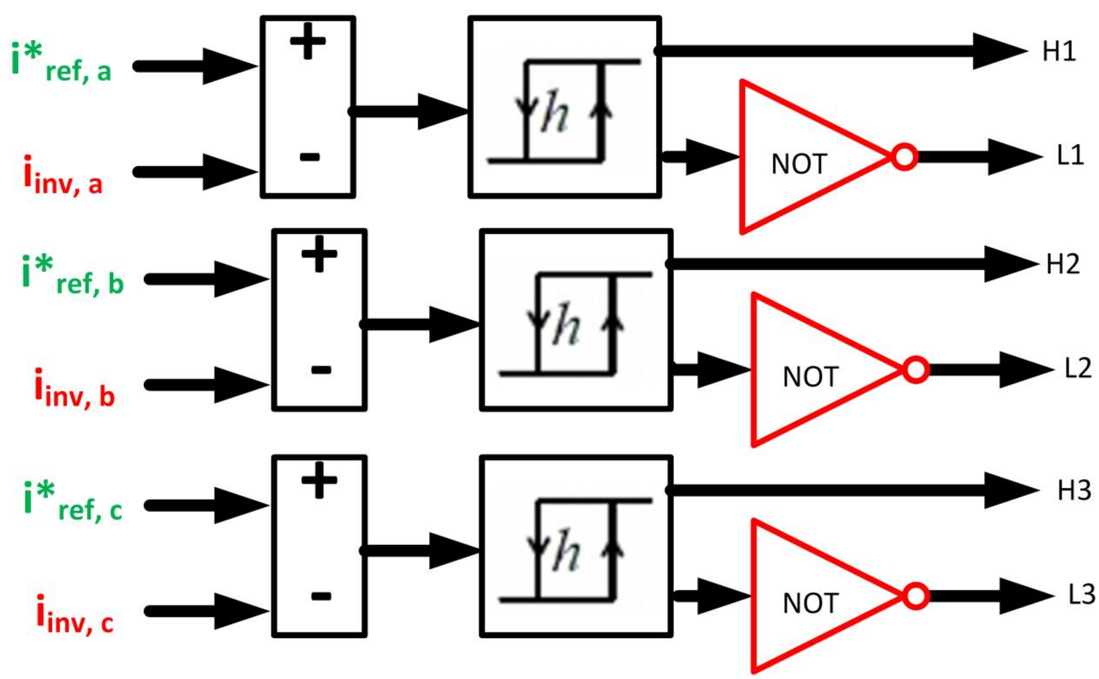

Figure 4- 16 : Functional diagram of Hysteresis current controller

4.10.1 Mathematical analysis of Hysteresis current controller

Hysteresis control mechanisms have been implemented in either analog or digital form. When the error between control references and control variables passes the positive or negative hysteresis band boundary, a considerable shift in the controller's output (switching state) occurs, as seen in Figure 4-16.

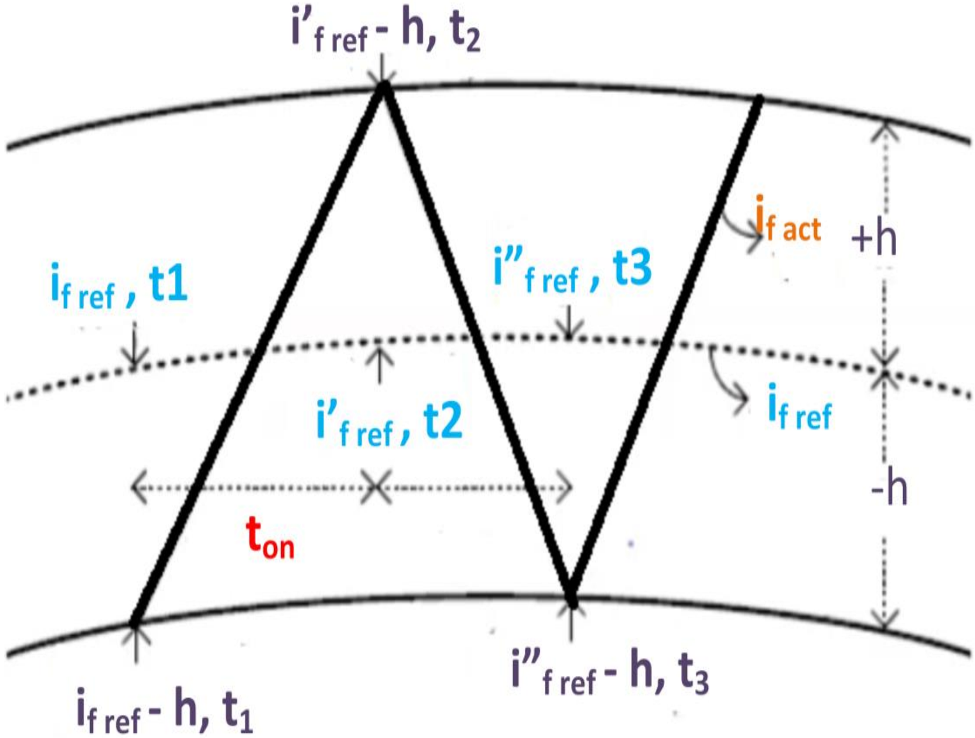

Figure 4- 17 : Hysteresis current control mechanisms

The inverter current $i_{inverter}$ is also known as line filter current i_{fact} . From Figure 4-17 , the reference current at time instant t_1 , t_2 , and t_3 are denoted as $i_{f_{ref}}$, $i'_{f_{ref}}$, and $i''_{f_{ref}}$, respectively. During on time, the derivative of filter current is represented, from the Figure 4-17, as:

$$\frac{di_{f_{act}}}{dt_{on}} = \frac{\left(i'_{f_{ref}} - i_{f_{ref}}\right) + 2h}{t_{on}} \tag{4.59}$$

During off time, the derivative of filter current is represented, from the Figure 4-17, as:

$$\frac{di_{f_{act}}}{dt_{off}} = \frac{\left(i''_{f_{ref}} - i'_{f_{ref}}\right) - 2h}{t_{off}} \tag{4.60}$$

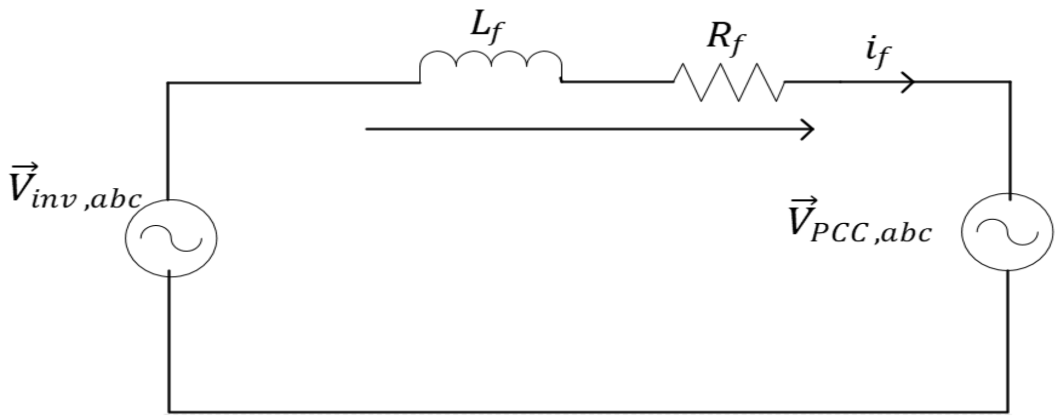

Figure 4- 18 : Functional diagram of grid tied system

According to KVL in the single line diagram of grid tied inverter, as shown in Figure 4-18, the inverter voltage can be computed as:

$$\vec{V}_{inv,abc} - \vec{V}_{PCC,abc} = R_f\vec{i}_{inv,abc} + L_f\frac{d\vec{i}_{inv,abc}}{dt}$$
$$= L_f\frac{di_f}{dt} + R_f\, i_f = L_f\frac{di_g}{dt} + R_f\, i_g \tag{4.61}$$

At the instant $t = t_{on}$, the equation (4.61) can be re-written as:

$$m_a\, V_{dc} - V_m \sin\omega t = L_f\frac{di_{f_{act}}}{dt_{on}} + R_f\, i_f \tag{4.62}$$

By substituting equation (4.59) into the equation (4.62), simplified inverter equation is represented as:

$$m_a\, V_{dc} - V_m \sin\omega t = L_f\{\frac{\left(i'_{f_{ref}} - i_{f_{ref}}\right) + 2h}{t_{on}}\} + R_f\, i_f \tag{4.63}$$

At time instant $t = t_{on}$, the voltage equation of grid tied inverter is represented as:

$$m_a\, V_{dc} - V_m \sin\omega t = L_f\{\frac{2h}{t_{on}}\} + R_f\, i_f \tag{4.64}$$

$$m_a\, V_{dc} - V_m \sin\omega t - R_f\, i_f = L_f\{\frac{2h}{t_{on}}\} \tag{4.65}$$

The voltage equation of grid tied inverter at off time is represented as:

$$-m_a\, V_{dc} - V_m \sin\omega t = L_f\frac{di_{f_{act}}}{dt_{off}} + R_f\, i_f \tag{4.66}$$

$$-m_a\, V_{dc} - V_m \sin\omega t = L_f\frac{\left(i''_{f_{ref}} - i'_{f_{ref}}\right) - 2h}{t_{off}} + R_f\, i_f \tag{4.67}$$

At time instant $t = t_{off}$, simplified inverter equation is represented as:

$$-m_a\, V_{dc} - V_m \sin\omega t = L_f\{\frac{-2h}{t_{off}}\} + R_f\, i_f \tag{4.68}$$

$$-m_a V_{dc} - V_m \sin\omega t - R_f i_f = L_f\{\frac{-2h}{t_{off}}\} \tag{4.69}$$

The on-time and off-time for grid tied inverter can be represented as:

$$t_{on} = \frac{2hL_f}{m_a V_{dc} - (V_m \sin\omega t + R_f i_f)} \tag{4.70}$$

$$t_{off} = \frac{2hL_f}{m_a V_{dc} + (V_m \sin\omega t + R_f i_f)} \tag{4.71}$$

The time period and switching frequency can be simplified as:

$$\begin{aligned} T_{period} &= \frac{1}{f_{sw}} = t_{on} + t_{off} \\ &= \frac{2hL_f}{m_a V_{dc} - (V_m \sin\omega t + R_f i_f)} + \frac{2hL_f}{m_a V_{dc} + (V_m \sin\omega t + R_f i_f)} \end{aligned} \tag{4.72}$$

The time period of PWM in context of line inductor, band size, and modulation index can be represented as:

$$T_{period} = \frac{1}{f_{sw}} = \frac{4hL_f}{m_a V_{dc}} \tag{4.73}$$

The line inductor can be represented as:

$$L_f = \frac{m_a V_{dc}}{4hf_{sw}} \tag{4.74}$$

The analogue controller maintains perfect current ripples inside the hysteresis range; however switching instances are not equal. A discrete system, on the other hand, has a preset sampling time, T_s. which it uses. Nonetheless, the hysteresis controller works only when $h > \frac{di_{f,max}}{dt} T_s$. When current ripples surpass ($h < \frac{di_{f,max}}{dt}$), the controller acts rather like a delta modulation scheme than hysteresis control.

The discrete controller requires 3.3 milliseconds (300 kHz) of sampling time to accurately reproduce the continuous hysteresis behavior. With a sampling time of 330 milliseconds (3 kHz), the operation of a discrete hysteresis controller is quite different from that of a continuous hysteresis controller. A low pass filter must be connected between the inverter and the grid since the output voltage of the inverter is non-sinusoidal (either a 2-level square pulse or a 3-level square pulse). Here, a passive low pass harmonic filter will be used to minimize voltage harmonics and current distortion. L or LC or LCL filters are all possibilities for this particular piece of equipment. For the whole frequency range, the L-type filters attenuate -20 dB/decade. A high inverter switching frequency is required when using an L filter to reduce high order harmonics effectively. This means that switching losses will grow with increasing frequency. Because the LC filters resonance frequency is affected by grid inductance, using a weak grid is not a good idea. Consequently, the LCL filter type is considered in the existing system. In addition to the frequencies -60 dB/decade attenuation over the resonance frequency, the LCL filter can be used with a reasonably low switching frequency for the provided harmonic attenuation.

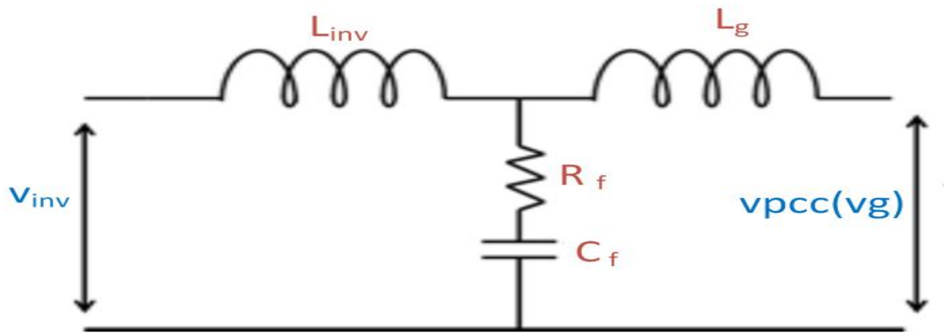

Figure 4- 19 : Basic block schematic of LCL type filter

The LCL circuit connection between the AC-terminal of single-stage PV system and the grid is shown in Figure 4-19. The output voltage of inverter and grid voltage are denoted as v_{inv} and v_{pcc}(or v_g). L_{inv} is the inverter side inductor and L_g is the grid side inductor; C_f is the filter capacitor and R_d is the damping resistor.

From the references [8][66][95][98][100], The line filter inductorL_{inv} can be computed as:

$$L_{inv} = \frac{V_{dc}\times(1-m_a)\times m_a}{4\times f_{switching}\times I_{rated}\times\Delta_{ripple}} \tag{4.75}$$

The relation between the line filter inductorL_{inv} and grid inductor $L_g$are represented as[8][66][95][98][100],:

$$L_g = \alpha L_{inv} \tag{4.76}$$

The current harmonics attenuation ratio (α) can be represented as[8][66][95][98][100],:

$$\alpha = 1 - \frac{\frac{1}{L_{inv} c_f \omega_{res}^2}}{\frac{\Delta_{ripple} V_{rated} \omega_0}{2\pi^2 V_{dc} f_{switching} \gamma}} \tag{4.77}$$

The filter capacitance can be computed as[8][66][95][98][100],:

$$C_f = \gamma C_{base\ capacitance} \tag{4.78}$$

The base capacitance and base impedance are computed as[8][66][95][98][100],:

$$C_{\text{base capacitance}} = \frac{1}{\omega_0 Z_{\text{base Impedance}}};$$
$$Z_{\text{base Impedance}} = \frac{V_g^2}{P_{\text{rated output power}}} \tag{4.79}$$

The damping resistance can be computed as[8][66][95][98][100],:

$$R_d = \frac{\omega_{res}}{C_f} \tag{4.80}$$

Hence, the resonance frequency for the PV system can be computed as[8][66][95][98][100],:

$$f_{res} = \frac{1}{2\pi}\sqrt{\frac{L_{inv}+L_g}{L_{inv}L_gC_f}} \tag{4.81}$$

Prior to selecting the LCL filter parameter, all necessary criteria must be fulfilled. Total filter inductances should be less than 0.1(p.u.) and the resonance frequency should be in the range of: $10\omega_g \leq \omega_{res} \leq \frac{\omega_{sw}}{2}$.

For the stability analysis of LCL filter, the transfer function without damping resistor can be computed as:

$$G(s) = \frac{1}{(L_{inv}L_gC_f)s^3+(\{L_{inv}+L_g\}C_f)s^2+(L_{inv}+L_g)s} \tag{4.82}$$

For the stability analysis of LCL filter, the transfer function with damping resistor can be computed as:

$$G(s) = \frac{1+R_dC_f}{(L_{inv}L_gC_f)s^3+(\{L_{inv}+L_g\}C_f)s^2+(L_{inv}+L_g)s} \tag{4.83}$$

By considering grid inductance L_2, the equation (4.83) is modified as:

$$G(s) = \frac{1+R_dC_f}{(L_{inv}(L_g+L_2)C_f)s^3+(\{L_{inv}+L_g+L_2\}C_f)s^2+(L_{inv}+L_g+L_2)s} \tag{4.84}$$

Figure 4-20 shows that the LCL filter has a higher attenuation level even at lower frequencies. The value of the resonance peak depends on the frequency of the system. Using the damping resistor as a resonance peak damper, as shown in Figure 4-21, reducing the resonance frequency by a factor of two while simultaneously increasing the grid inductance's impact on resonance frequency values is possible. When grid impedance varies, we must thus monitor it constantly and shut off the inverter system if it goes outside a specified range.

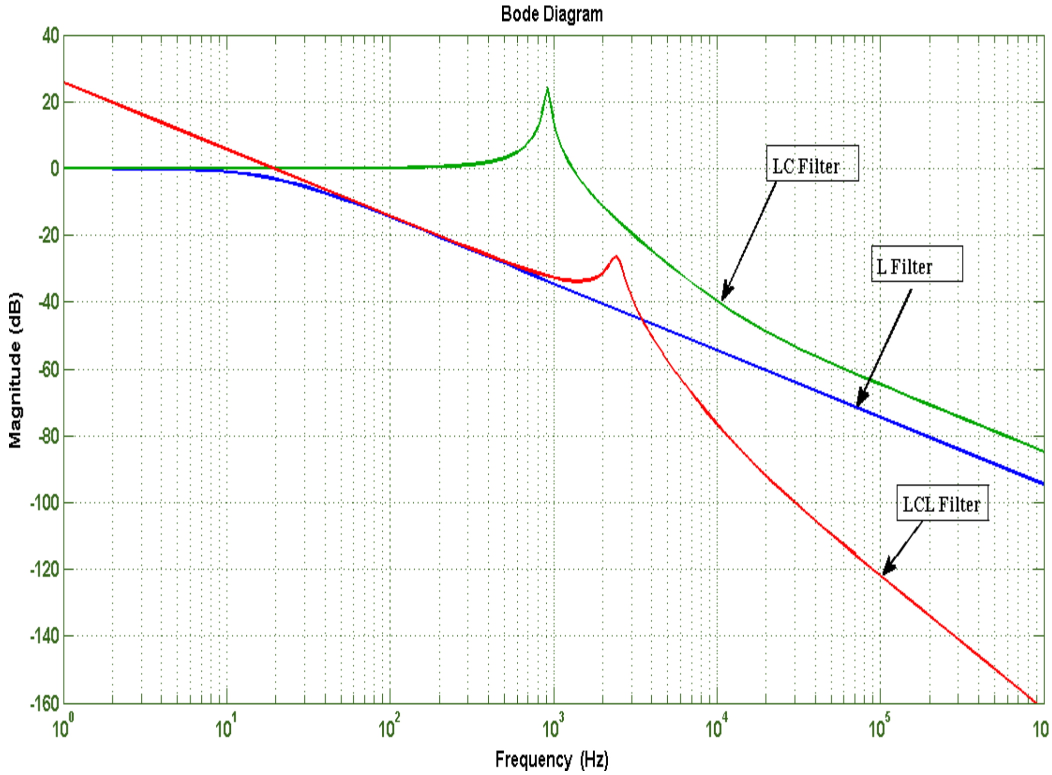

Figure 4- 20 : Bode Plots for general filter variants

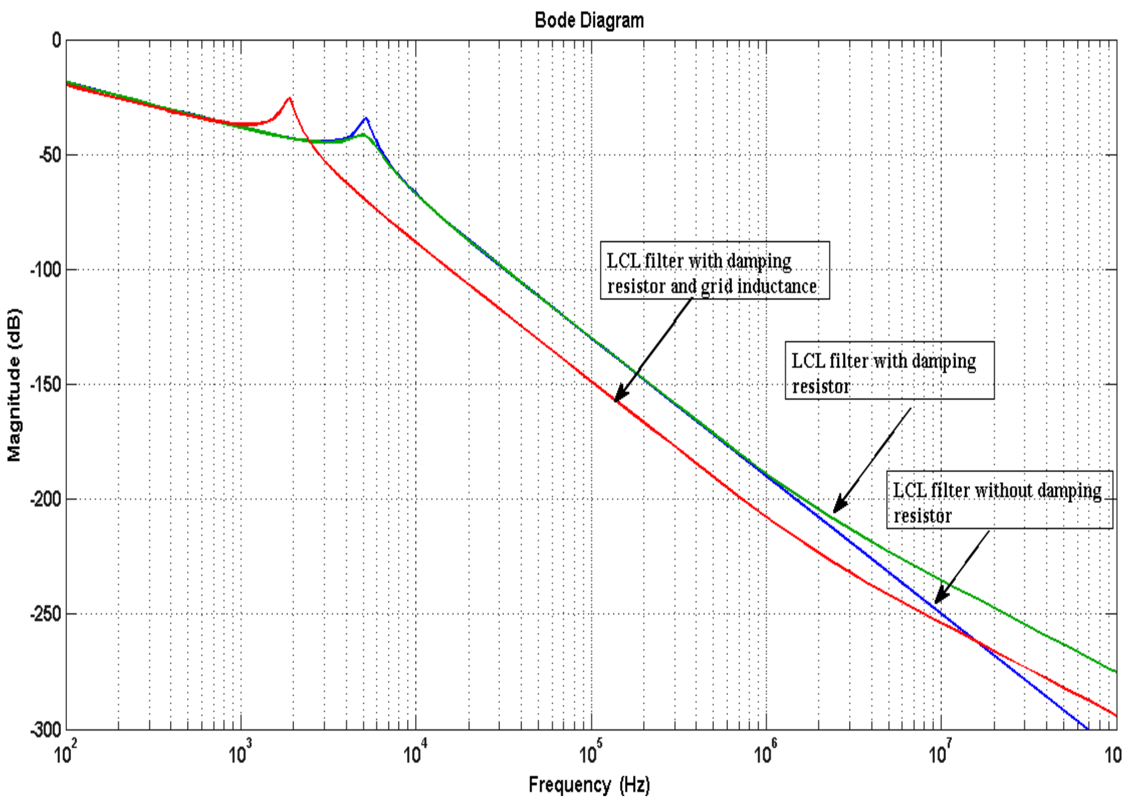

Figure 4- 21 : Bode plot for LCL type filter considering different conditions

4.10.2 Reference Current Generation using instantaneous power Theory

The compensation scheme described here can be used to either a three-phase, three-wire system or a three-phase, four-wire system. However, in either situation, the aim is to provide balanced supply current so that the zero sequence component of the current is zero in both cases and described below:

$$i_{s_a} + i_{s_b} + i_{s_c} = 0 \tag{4.85}$$

Because it is assumed that the power factor angle is zero, it follows that the instantaneous reactive power delivered by the source is also zero. When this angle is greater than zero, on the other hand, the source gives reactive power which is equals to tan $\frac{\varphi}{3}$ times the amount of instantaneous power, where φ is phase angle between source voltage and source current.

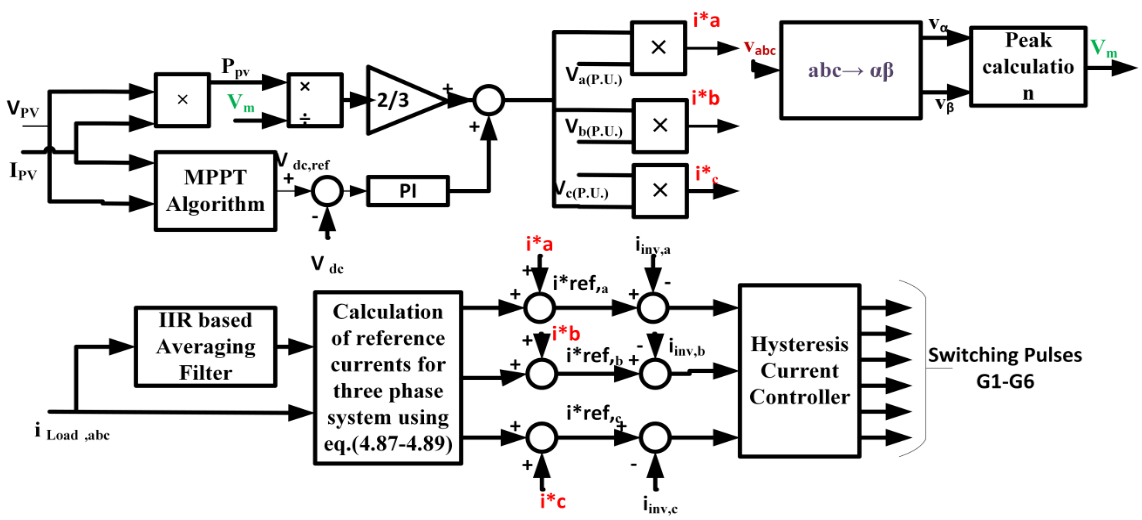

Figure 4- 22 : Control mechanism of single stage grid tied PV system in abc reference frame

In a balanced three-phase circuit, the instantaneous power is constant, however in an unbalanced circuit; the instantaneous power has a double frequency component in addition to the dc value. This is accomplished by the use of a voltage source converter, which delivers the double frequency component such that the source supplies the dc value of the load power. The active power of load can be computed as:

$$v_{s_a}\, i_{s_a} + v_{s_b}\, i_{s_b} + v_{s_c}\, i_{s_c} = P_{Load_{avg}} \tag{4.86}$$

It is possible to determine the average load power by employing a moving average (MA) filter with an averaging time of half a cycle. The harmonic component in the load current does not require any real power to be supplied by the source current. The role of inverter is activated at the end of a single cycle of operation. Moreover, at the end of three cycles, the inverter operates at unity power factor mode.

The AC components of load currents are computed as:

$$\tilde{i}_{Load_a} = i_{Load\,a} - i_{Load_{avg,\ a}} \tag{4.87}$$

$$\tilde{i}_{Load_b} = i_{Load\,b} - i_{Load_{avg,\ b}} \tag{4.88}$$

$$\tilde{i}_{Load_c} = i_{Load\,c} - i_{Load_{avg,\ c}} \tag{4.89}$$

The reference values of currents for the hysteresis current controller are computed as:

$$i^*_{ref\ a} = \tilde{i}_{Load_a} + \left(P_{loss} + \frac{2V_{PV}I_{PV}}{3V_m}\right)\frac{v_a}{V_m} \tag{4.90}$$

$$i^*_{ref\ b} = \tilde{i}_{Load_b} + \left(P_{loss} + \frac{2V_{PV}I_{PV}}{3V_m}\right)\frac{v_b}{V_m} \tag{4.91}$$

$$i^*_{ref\ c} = \tilde{i}_{Load_c} + \left(P_{loss} + \frac{2V_{PV}I_{PV}}{3V_m}\right)\frac{v_c}{V_m} \tag{4.92}$$

The error between the reference value of DC-bus and actual value of DC-bus is computed in the equation (4.93). The P_{loss} is computed in the equation (4.94) for extracting the active power from PV panels.

$$\varepsilon(n) = V_{dc_{ref}}(n) - V_{dc}(n) \tag{4.93}$$

$$P_{loss} = V_{dc}(n) + K_P\,[\varepsilon(n) - \varepsilon(n-1)] + K_i\,T_s\,\varepsilon(n) \tag{4.94}$$

$$v_{a_{P.U}} = \frac{v_a}{V_m}\ ;\ v_{b_{P.U}} = \frac{v_b}{V_m}\ ;\ v_{c_{P.U}} = \frac{v_c}{V_m}\ ; \tag{4.95}$$

Prior to the connection of the PV system, both the load power and the source power have the same magnitude and are oscillatory in their output. The supply power becomes flat as soon as the inverter is connected, and delivers the oscillating component after it has been linked. Because the action of the PV system is immediate, it should be highlighted that optimal current sources are used to achieve desire result. Once the load is altered to balanced values at 0.5 s, the source and load powers become flat, and the inverter power and neutral voltage both become zero as a result of the change.

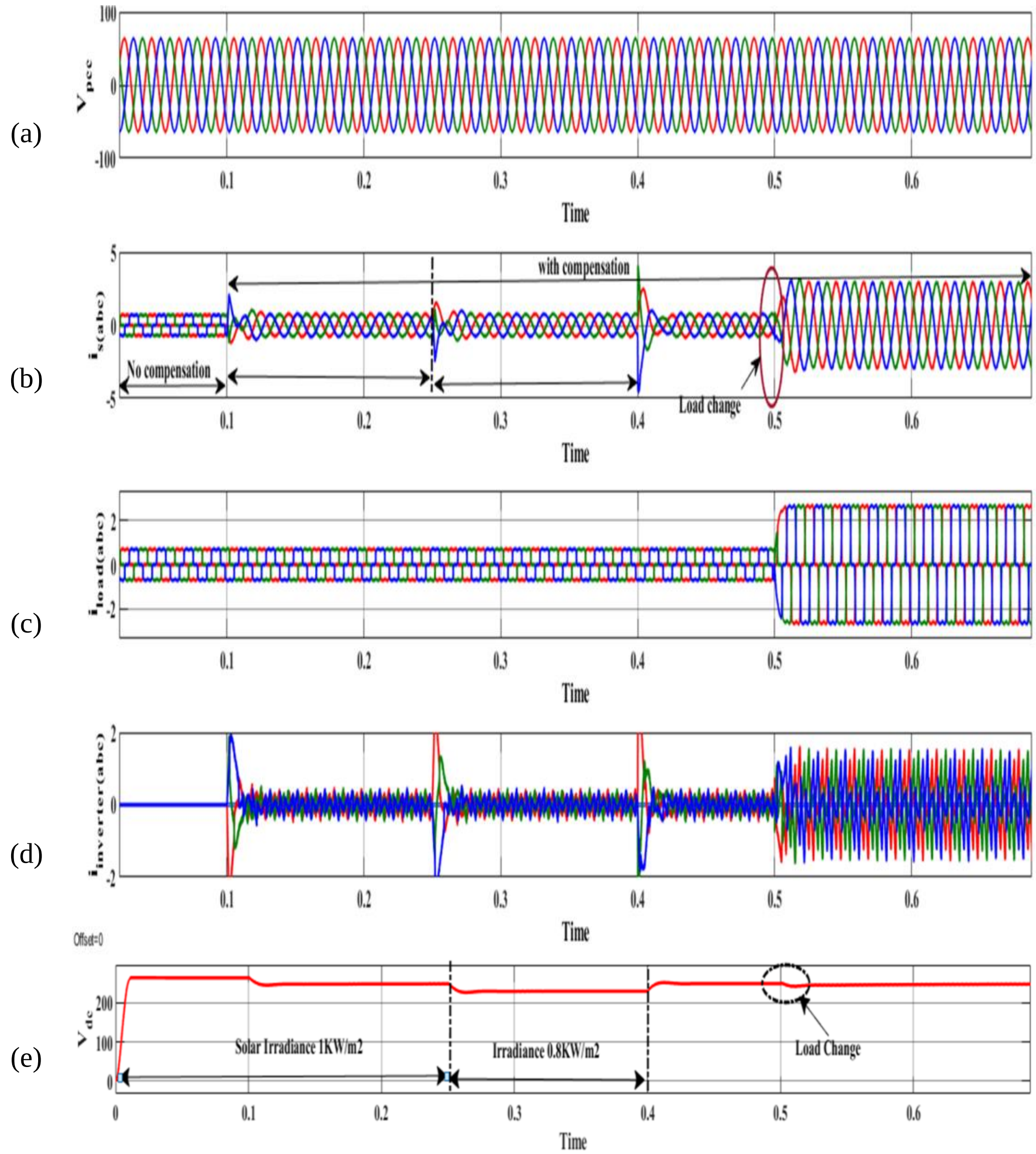

Figure 4- 23 : Simulation result of Multipurpose PV system connected to non-linear load at PCC (a) PCC voltage, (b) grid currents, (c) inverter currents, (d) load currents, and (e) DC-bus voltage

This is demonstrated in Figure 4-23, which depicts the three source voltages and currents, as well as the inverter currents, respectively. The operation of the source at unity power factor, as well as the balancing of source currents, may be seen in Figure 4-23(a) and (b). According to Figure 4-23(e) when the solar irradiance is changed, the inverter is operative in same manner while when load is shifted that time inverter currents become balanced as a result of the load being balanced, as observed in

Figure 4-23(c) and (d).The operation of the inverter when it is turned on in 20 milliseconds is immediate because it is created from ideal current sources, which is something to keep in mind. Furthermore, because of the load inductances, when the load is changed, the transients last around 2 cycles before they die out. The voltage source converter(PV inverter) has no influence on the amount of time required by the load to settle. It should be noted that after the PV inverter is attached, neither the load power nor the neutral voltage change.

4.11 Current-Sensor less MPPT In Grid-tied Photovoltaic System

Reference (87) presented their works on current-sensor less power-angle based MPPT control for single-stage grid-connected System. The voltage source inverters with current sensors and power angle based MPPT; these researchers had proposed a novel quantity for current-sensor less power-angle based MPPT (VSIs). The suggested control scheme, which MPPT eliminates the need of current sensor and instead relies solely on a voltage sensor: Instead of measuring current, the sine value of the power-angle sensor (the phase angle between the inverter output voltage and the power grid voltage) is computed for MPPT. The usage of current sensors accounts for a significant portion of the costs and complexity challenges (such as failure in currents sensor, calibration error of sensor, quantization error of ADC etc.) associated with MPPTs during failure in currents sensor. By taking into account the hardware cost and the simplicity, control system of grid connected PV system had given satisfactory performance.

4.11.1 Conceptual framework and description of Current-Sensor less MPPT in Grid-tied Photovoltaic System

The control system of PV system is capable to exchange active and reactive power to the utility. The MPPT algorithm is a part of controls system, which is employed to extract maximum power from PV panels and injected to utility through inverter. Figure (4-4) of section 4.3 indicates that in order to calculate the maximum power point of a PV panel, both voltage and current must be known. The maximum amount of power can be extracted by sensing voltage and current in real time. During the day, the PV system's output voltage is stable throughout its operational range. As a result, the power injected by PV inverter (P_{inv}) is inversely proportional to the current variation. Modified-MPPT can be achieved from a PV system if a correlation can be established between the PV current and the output AC current (which is being detected to build a close loop).AC currents and DC link voltage are used in the MPPT algorithm (instead of the PV current).

4.11.1.1 Mathematical analysis of sine-angle based MPPT for Single-Stage PV system

There is an equivalent diagram of a grid-connected generation system in Figure4-24 to describe the power injection principle from a generator into the electricity grid. Figure 4-24(b) shows a vector diagram of how output currents can be utilized to build a PV current reference that can be used in the MPPT method to calculate maximum power. As a result of this research, a constant multiplication factor has been developed between PV current and AC current for any given available power. Thus, using the available current reference and PV voltage, the maximum power may be determined.

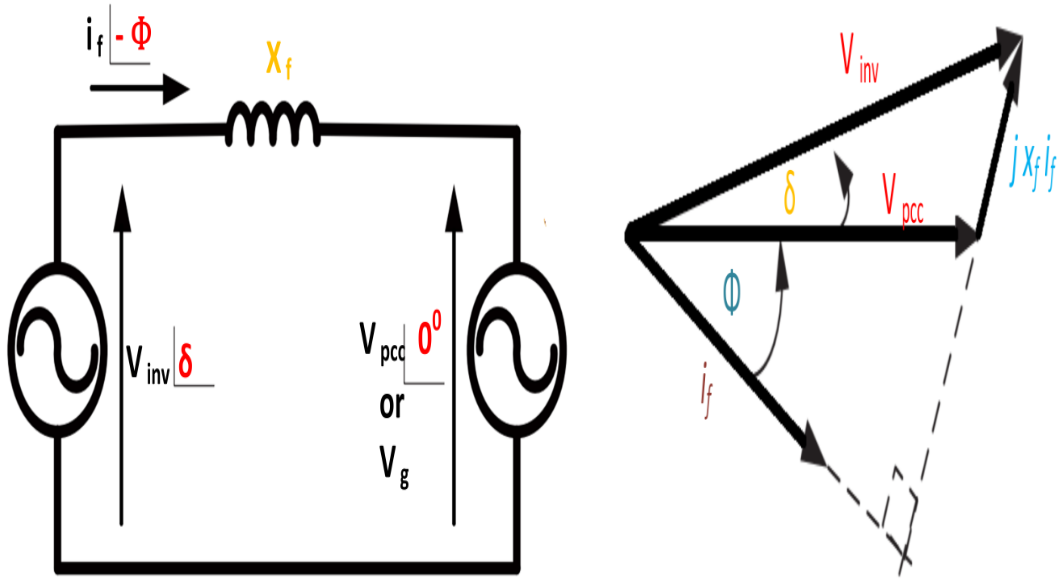

Figure 4- 24 : Functional and Phasor diagram of grid tied PV system during power injection into a grid

From phasor diagram shown in the figure 4-24, the active and reactive power of grid tied system, are computed as:

$$P_{inv} = \frac{v_{inv} v_{pcc} \sin\delta}{X_f} \tag{4.96}$$

$$Q_{inv} = \frac{v_{pcc}^2 - v_{inv} v_{pcc} \cos\delta}{X_f} \tag{4.97}$$

The relationship of inverter voltage, modulation index, and DC-bus voltage or PV panel voltage is described as:

$$v_{inv} = m_a \frac{V_{DC}}{2} = m_a \frac{V_{PV}}{2} \tag{4.98}$$

The Power of PV panels can be described as:

$$P_{PV} = V_{PV} \times I_{PV} \tag{4.99}$$

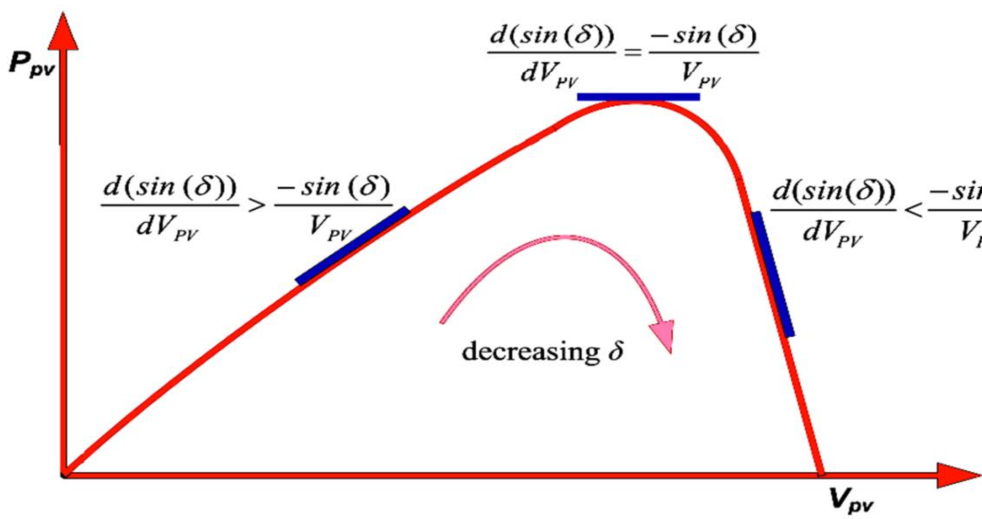

Figure 4- 25 : Power curve for PV panel using sin angle based DC current sensor-less MPPT

The DC link voltage or PV voltage is directly proportional to inverter voltage (i.e.$V_{PV} \propto v_{inv}$)by considering following terms as constant terms : grid voltages, filter reactance, modulation index, and hardware configuration. The active power relation given in equation is re-written as:

$$P_{inv} \propto (V_{PV} \times \sin\delta) \tag{4.100}$$

The sine value of the power-angle ($\sin\delta$) can be used to substitute the PV current in order to inject maximum power through inverter to grid using a modified-MPPT algorithm[87].

4.11.1.2 Modified-INC MPPT algorithm

The basic principles of the INC MPPT algorithm can be summarized thusly: According to the PV module power curve illustrated in Figure (4-4) and Figure (4-25), the derivative of PV module power P_{PV} with respect to its voltage is positive prior to reaching the MPP, then zero, and then negative after passing through the MPP.

$$\frac{dP_{PV}}{dV_{PV}} \propto \left\{\frac{d((V_{PV} \times \sin\delta))}{dV_{PV}}\right\} \propto \{(V_{PV} \times \frac{d(\sin\delta))}{dV_{PV}} + (\sin\delta)\} \quad (4.102)$$

The P_{PV} derivation is given in equation (4.102), which results error (e) signal. It is given as

$$e = \frac{d(\sin\delta))}{dV_{PV}} + \frac{\sin\delta}{V_{PV}} \quad (4.103)$$

It is then possible to keep track of the maximum power point by watching the actuating error, then following the following rule:

$$\delta(n) = \begin{cases} \delta(n-1) + \Delta\delta, & e < 0 \\ \delta(n-1) - \Delta\delta, & e \geq 0 \end{cases} \quad (4.104)$$

Using the modified INC approach [86-92] , the slope of the PV array power curve vs voltage is zero at the maximum power point (MPP) of the array. The accuracy requirements at steady state and the MPPT response time dictate the size of the iteration step for the INC MPPT algorithm. It is therefore necessary to evaluate a trade-off between dynamic and steady-state reactions at the corresponding design stage.

4.12 Modified DC Current-Sensor less MPPT for Grid-tied Photovoltaic System in Synchronous reference frame

Power of photovoltaic system ought to be equal to the output power of inverter at the VSI AC-side terminals, which is equal to the grid power, omitting the inverter loss and filter power loss, based on the power balance of both inverter sides in steady condition.

$$\mathrm{P_{PV}}(= \mathrm{V_{PV}} \times \mathrm{I_{PV}}) = \mathrm{P_{inv}}\ (= \frac{3\mathrm{V_d I_d}}{2}) \quad (4.105)$$

The power of the PV panels is directly proportional to ac current component d-axis coordinate ($\mathrm{P_{PV}} \propto \mathrm{i_d}$)by considering following terms as constant terms : balanced grid voltages(v_d = constant), fine grid synchronization ($v_q = 0$), constant filter reactance. It is described as:

$$P_{PV} \propto I_d \tag{4.106}$$

The power variation of PV panels P_{PV} with voltageV_{dc} is calculable as follows:

$$\frac{dP_{PV}}{dV_{dc}} = \left\{\frac{3}{2}\frac{d(V_d I_d)}{dV_{PV}}\right\} = \left\{V_d \frac{3}{2}\frac{d(I_d)}{dV_{PV}}\right\} + \left\{I_d \frac{3}{2}\frac{d(V_d)}{dV_{PV}}\right\} \tag{4.107}$$

For the balanced grid voltages, d-axis component of voltage vector is constant and equation is simplified as:

$$\frac{dP_{PV}}{dV_{dc}} = \left\{V_d \frac{3}{2}\frac{d(I_d)}{dV_{PV}}\right\} \propto \frac{d(I_d)}{dV_{PV}} \tag{4.108}$$

At kth sample, the DC-link voltage and d-axis inverter current are computed as:

$$\Delta V_{dc}(k) = V_{dc}(k) - V_{dc}(k-1) \tag{4.109}$$

$$\Delta i_d(k) = i_d(k) - i_d(k-1) \tag{4.110}$$

When $I_d \neq 0$, it means there is change in climate condition. According to equation (4.108), if $\Delta I_d > 0$, then $\frac{\Delta I_d}{\Delta V_{dc}} > 0$,and the MPPT reference voltage is increased to bring the operating point towards the maximum power point. The reference voltage $V_{dc_{ref}}(k)$ for outer voltage control loop is computed by modified MPPT algorithm as per the equation.

$$V_{dc_{ref}}(k) = \begin{array}{c|c} V_{dc_{ref}}(k) + \Delta V_{step-size} & \begin{array}{c}(\Delta I_d > 0 \& \Delta V_{dc} > 0) \\ ||(\Delta I_d < 0 \ \& \Delta V_{dc} < 0)\end{array} \\ \hline V_{dc_{ref}}(k) - \Delta V_{step-size} & \begin{array}{c}(\Delta I_d < 0 \& \Delta V_{dc} > 0) \\ ||(\Delta I_d > 0 \& \Delta V_{dc} < 0)\end{array} \end{array} \tag{4.111}$$

While$\Delta I_d < 0$, then $\frac{\Delta I_d}{\Delta V_{dc}} < 0$,and the MPPT reference voltage must be decreased in order to bring the operating point toward the maximum power point, as shown in Figure 4-26. The MPPT's step size affects how quickly the MPP is monitored.

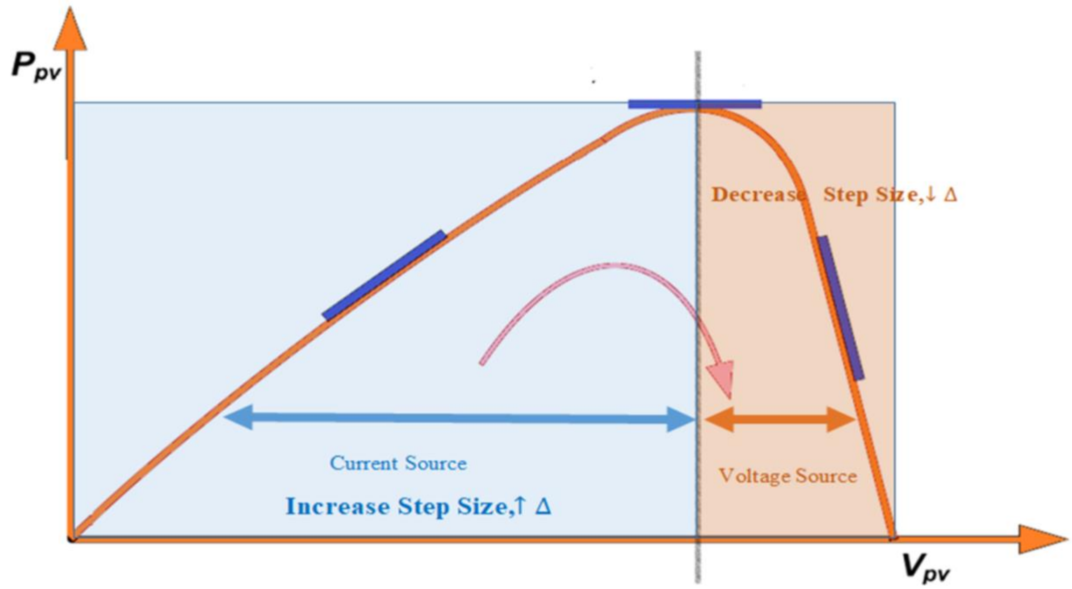

Figure 4- 26 : Power curve for PV panel using modified dc current sensor-less MPPT

.

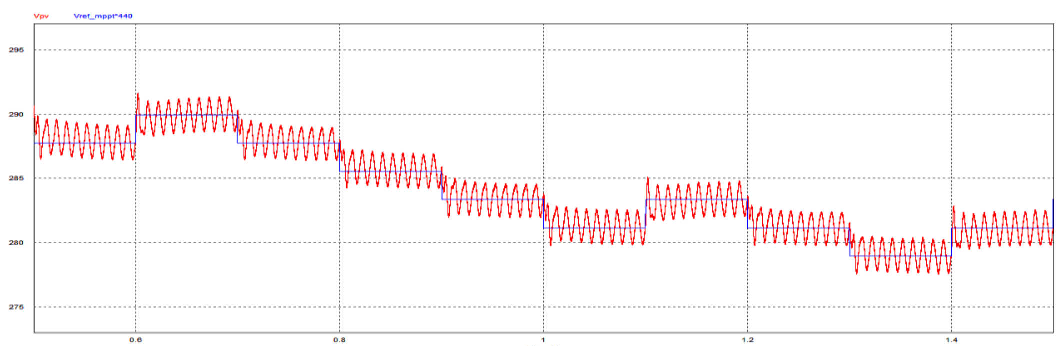

Figure 4- 27 : Tracking the change in V_{PV} [Upper Trace: Voltage Generated by PV Array (Red): X axis: 1 Div. = 20 mSec, Y axis : 1 Div. = 5 V; Lower Trace: Reference Voltage Generated by MPPT Algorithm (Blue): X axis : 1 Div. = 20 mSec, Y axis : 1 Div. = 5 V]

In order to get faster tracking, one can use larger increments, however the system may not run at the MPP perfectly, instead oscillating around it, and this results in low efficiency. When the MPPT is set to a small increment, the situation is the opposite. For the fixed step-size MPPT, a trade-off between dynamics and oscillations is necessary. Here, Figure 4-27 depicts the PV voltage generated by PV Panels tracks MPPT reference generated by modified DC current sensor-less MPPT algorithm.

Now from Figure 4-27,it can be seen that MPPT reference voltage tracks the PV panel voltage accurately. From this the behavior of the algorithm at the standard temperature (25^{o}C) and irradiation (1000 $\frac{W}{m^2}$) can be analyzed. According to the error generated by MPPT voltage reference and sensed PV array voltage is fed to PI controller of outer voltage control loop , which determines active current will be injected to utility grid and constant DC link voltage is maintained.

(a)

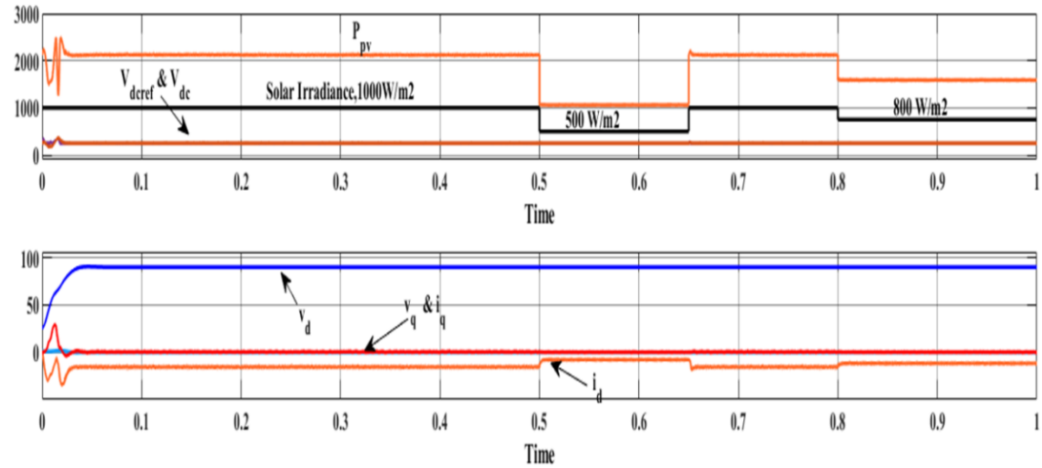

(b)

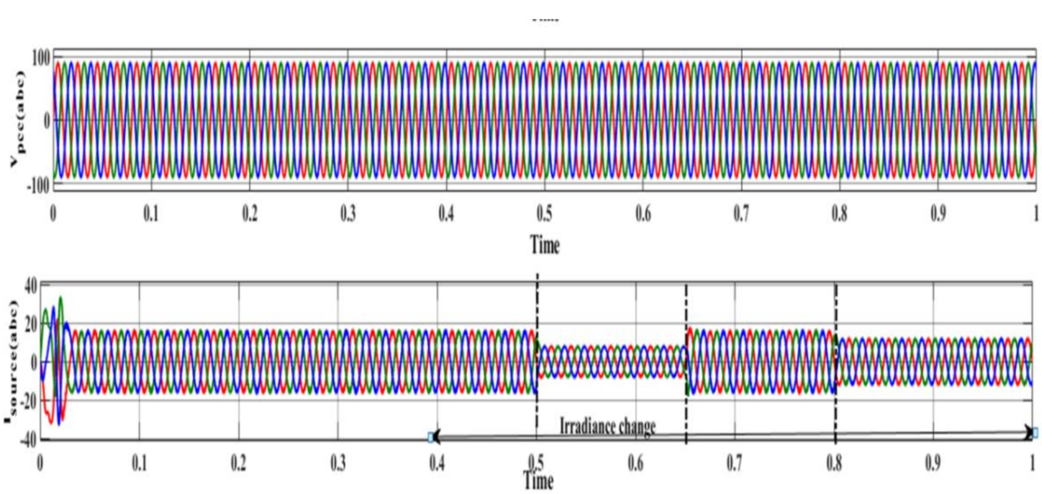

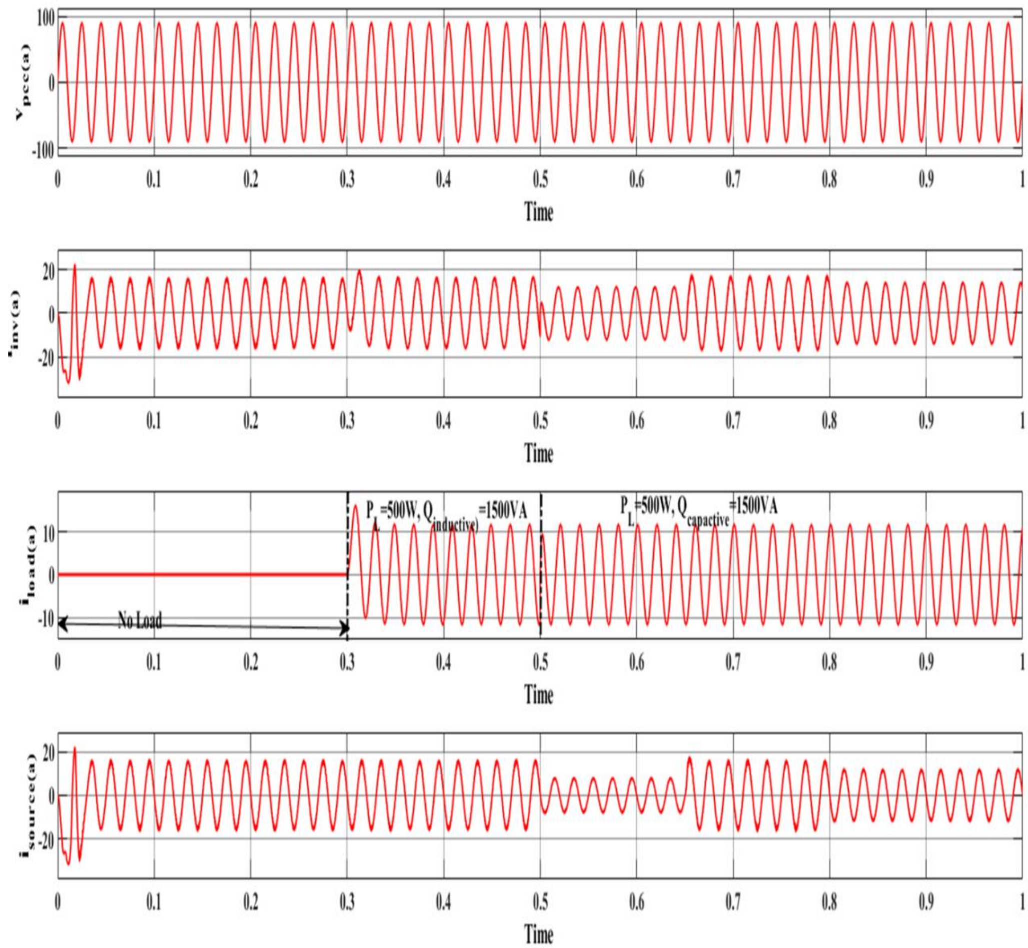

(c)

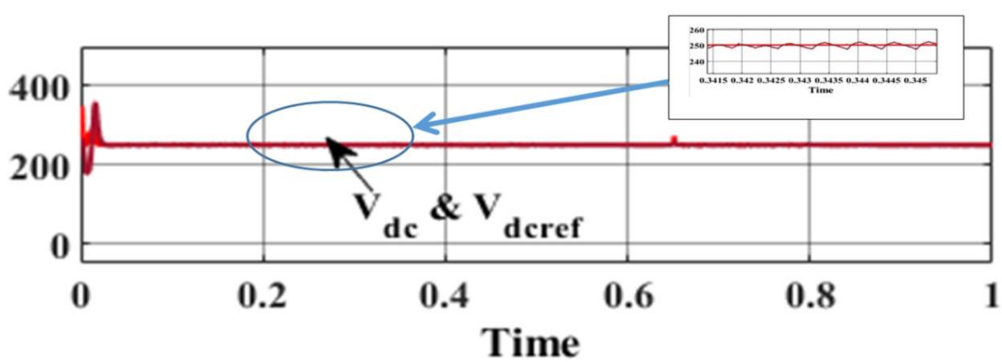

(d)

Figure 4- 28 : Dynamic performance of Multipurpose PV system using a modified DC current sensor-less MPPT and synchronous frame current control

Figure 4-28 (a) illustrate the variation in solar power P_{PV} as per the variation in solar irradiance. The solar isolation/irradiance is varied from 1000 $\frac{W}{m^2}$ to 500 $\frac{W}{m^2}$ from time instant t =0.5 to t =0.65 seconds, again to 800 $\frac{W}{m^2}$ from time instant t =0.65 to t =0.8

seconds, and further shifted to 1000 $\frac{W}{m^2}$at t =0.8 seconds, depicted in Figure 4-28 (a). Figure 4-28(a) also demonstrate voltages and currents in dq reference frame. Figure 4-28(b) demonstrate that the utility grid is only interfaced with PV inverter up-to time instant t=0.3 seconds, then inductive load is connected at point of common coupling from time instant t = 0.3 to 0.5 seconds, and load shifted to capacitive load after time instant t= 0.5 seconds, as . From simulation results depicted in the Figure 4-28(b) and (c) , it is observed that the multipurpose PV system inject only active power (2500W)into utility grid at maximum power point using modified MPPT algorithm at time instant t $\leq$ 0.3 seconds. At time instant between t= 0.5 seconds and t = 0.65seconds, the active power decreased due to abrupt change in solar irradiance from 1000 $\frac{W}{m^2}$ to 500$\frac{W}{m^2}$. While, the active power increased due to increase in solar irradiance from 500 $\frac{W}{m^2}$ to 1000 $\frac{W}{m^2}$ again at time instant between t= 0.65 seconds and t = 0.8seconds, as depicted in Figure 4-28. The modified DC current sensor-less MPPT algorithm uses sensed DC-bus voltage and d-axis ac current component of inverter for computing direction in which step size is added to reach maximum power point, as depicted in Figure 4-28. The variation in d-axis current component of inverter in synchronous frame is directly influence by change in solar irradiance, which fact is utilized to employ DC current sensor-less MPPT algorithm, as depicted in Figure 4-28. From the simulation result as well as mathematical analysis, it is concluded that maximum power point extracted from PV panel is possible without using dc current sensor.

4.13 Conclusion

This chapter discussed modeling a multipurpose single-stage grid-tied PV system using Simulink/MATLAB. The single-stage grid-tied PV system at PCC serves various purposes and is connected to the utility grid and multiple reactive loads. A single-stage grid-tied PV system conventional control is adjusted to inject active power into the grid together with reactive power support to accomplish either unity power factor at utility or PCC to operate as Partial PV & Partial-STATCOM or Full STATCOM mode, depending on the system's requirements. The partial STATCOM operation mode control objectives include power factor correction, voltage regulation, and reactive power management. For complete STATCOM operation, the primary goal of control is voltage control. The software simulation studies have verified the controller performance in both modes of operation. If the controller is in partial STATCOM mode, it provides reactive power to the load in order to keep the grid power factor at unity. For demonstration purposes, voltage control modifies the photovoltaic system's active power output to demonstrate the successful decoupling of the active and reactive power controllers. When a load is abruptly applied, the controller disconnects the solar panels from the inverter and manages the voltage using the inverter's full capability. The single-stage grid-tied PV system is designed and simulated using a modified DC current sensor without MPPT to attain the desired performance.